







# Bayesian estimation of the maximum magnitude $M_{max}$ based on the statistics of extremes

*Work Package 5 "PSHA"*



AUTHORS		REVIEW		APPROVAL	
Name	Date	Name	Date	Name	Date
<i>I. Zentner</i>		<i>I. Main / J. Douglas</i>		<i>E. Viallet</i>	
	2018/05/14	 	2018/12/03		2018/12/21
				Public-access 	
				SIGMA-2 restricted 	

## Document history

DATE	VERSION	COMMENTS
2018/05/14	0	
2018/09/15	1	<i>Revision after SIGMA-2 scientific committee review</i>

## Executive summary

Probabilistic Seismic Hazard Assessment (PSHA) has the goal to evaluate annual frequencies of exceeding a given ground motion Intensity Measure such as PGA (Peak Ground Acceleration), PSA (Pseudo Spectral Acceleration) etc. For this purpose, it is necessary to describe occurrence rates of earthquakes and the distribution of their magnitudes. The most popular distribution of magnitudes is the exponential distribution from the Gutenberg-Richter (GR) law. Numerous studies and applications showed that the GR distribution is pertinent to model the distribution of magnitudes in the lower and moderate magnitudes ranges. However, it deviates from the log-linear model in the higher frequency range. For this reason and to account for finite energy of faults, the GR distribution is generally truncated at a maximum possible magnitude value  $m_{max}$ . The justification of the choice of  $m_{max}$  from physics or simple statistics is not straightforward. Concurrently, recent analyses showed that the maximum magnitude can have a major impact on the hazard curve when high return periods as required for safety analysis of NPP (20 000 years) are considered.

This report addresses the estimation of the maximum magnitude in the truncated GR law by means of a Bayesian approach involving extreme value statistics. The Bayesian updating approach allows for the combination of different sources of information and to overcome the bias of the simple maximum likelihood estimator. The development of the prior distribution of maximum magnitude relies on drawing analogies to tectonically comparable regions to increase the dataset for the development of generic distribution that can be updated for particular configurations. This is achieved by the likelihood function. When Poissonian occurrence of earthquakes is assumed, then the maximum magnitude  $m_{max}$  as well as its probability distribution (linked to epistemic uncertainty) can be estimated by deriving the extreme value distribution analytically. We propose a new method to construct the likelihood function based on the distribution of extremes of the truncated GR law. The proposed method constitutes an improvement of former developments by EPRI, see Johnston (1994), and further promoted by USNRC (2012) where the Bayesian updating approach is used to account for prior information from similar tectonic zones and expert judgment. In the proposed method, only the completeness period of  $m_{maxobs}$  is required, so that there is no need to determine and use the exact completeness periods for magnitude bins of smaller events and to introduce the associated uncertainties. This makes the approach easy to implement and to apply.

The proposed method is more rigorous and outperforms the EPRI/USNRC Bayesian updating approach in terms of precision. As for the EPRI method, the approach allows addressing the case where  $m_{maxobs}$  is outside its completeness interval. The analyses conducted in this report with simulated catalogues demonstrated the capability of the Bayesian updating approach to correctly estimate  $m_{max}$  for periods of observation available in France. It is acknowledged here that the analytical expressions of extreme value distributions can be derived as long as Poisson occurrence is assumed (the magnitude distribution can be the GR law or any other).

## Table of content

Document history .....	2
Executive summary.....	2
Introduction.....	4
1. Short literature review .....	6
2. Extreme value distributions .....	8
Generalized extreme value distribution .....	8
Generalized Pareto distribution (GPD).....	10
Implication on earthquake recurrence and extreme magnitudes .....	11
Poisson model for earthquake recurrence.....	14
The Gutenberg-Richter magnitude distribution and associated extreme value distribution .....	14
3. Estimation of maximum magnitude by means of Bayesian approach using the extreme value distributions .....	16
Bayesian updating.....	16
Different ways to express the likelihood function based on the distribution of extremes .....	16
EPRI method.....	19
4. Application and case studies .....	20
French macrozones.....	21
Prior distribution .....	22
Analyses conducted with simulated catalogues.....	23
Analyses with data from FCAT17 catalogue.....	31
Accounting for uncertainty in the data from FCAT17 catalogue .....	34
5. Conclusion and Perspectives .....	38
6. References .....	39
APPENDIX 1.....	43
Visualization of the data from all 6 macrozones.....	43
APPENDIX 2.....	45
GR law in log10 base .....	45

## Introduction

Probabilistic Seismic Hazard Assessment (PSHA) has the goal to evaluate annual frequencies of exceeding a given ground motion Intensity Measure (IM) such as PGA (Peak Ground Acceleration), PSA (Pseudo Spectral Acceleration) etc. For this purpose, it is necessary to describe occurrence rates of earthquakes and the distribution of their magnitudes. This is the step 2 in the **Figure 1**. The methodology is illustrated in the same figure. PSHA is conducted in four steps as illustrated in the figure: it starts with earthquake source (1), recurrence (2) and ground motion (3) modeling and combines this information (4) to evaluate exceedance probabilities. The latter are determined as a function of IM by the hazard curve.

$$P_Y(Y > y) = \sum_{i=1}^{N_s} \lambda_i(M \geq m_{min}) \int_{m_{min}}^{m_{max}} \int_{r_{min}}^{r_{max}} P_i(Y > y|m, r) f_i(m) f_i(r) dr dm \quad (1)$$

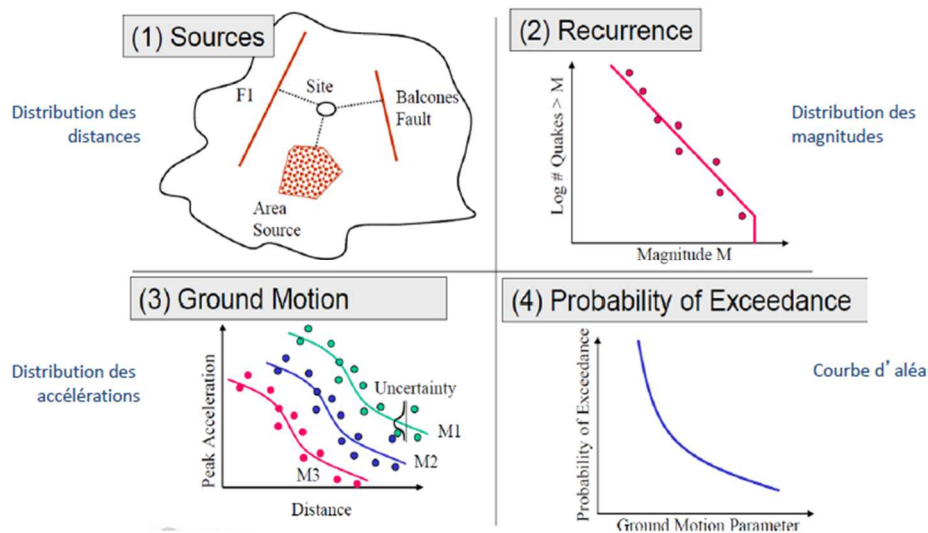


**Figure 1:** PSHA methodology.

The hazard integral, equation (1), is evaluated for magnitudes in the range  $m_{min}$  and  $m_{max}$ , where  $m_{max}$  is the maximum magnitude that can be expected for a given site. It is also generally acknowledged that the hazard integral has to be bounded by a minimum magnitude  $m_{min}$  below which no considerable impact on structures can be expected. The distribution of magnitudes  $f(m)$ , evaluated in step 2 of Figure 1, allows for a characterization of seismic activity for each zone or source. The most popular distribution of magnitudes is the exponential distribution from the Gutenberg-Richter (GR) law. The maximum magnitude  $m_{max}$  is the upper value used to truncate the GR law. Numerous studies and applications showed that the GR distribution is a good choice to model the distribution of magnitudes in the lower and moderate magnitudes ranges. However, it deviates from the log-linear model in the higher frequency range. To account for finite energy of faults, the GR distribution is generally truncated at  $m_{max}$ , see **Figure 2**. The figure represents the normalized number of annual exceedances of magnitudes  $m$ .

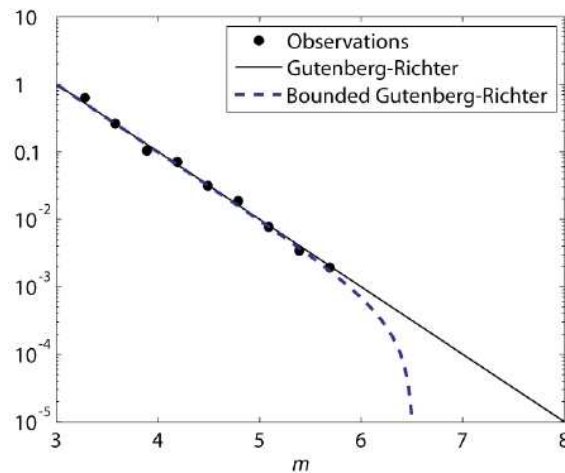


**Figure 2:** Cumulative frequency-magnitude distribution, normalized to the number of events above magnitude 3, illustrating the GR law and truncated or bounded GR law considering finite  $m_{max}$ .

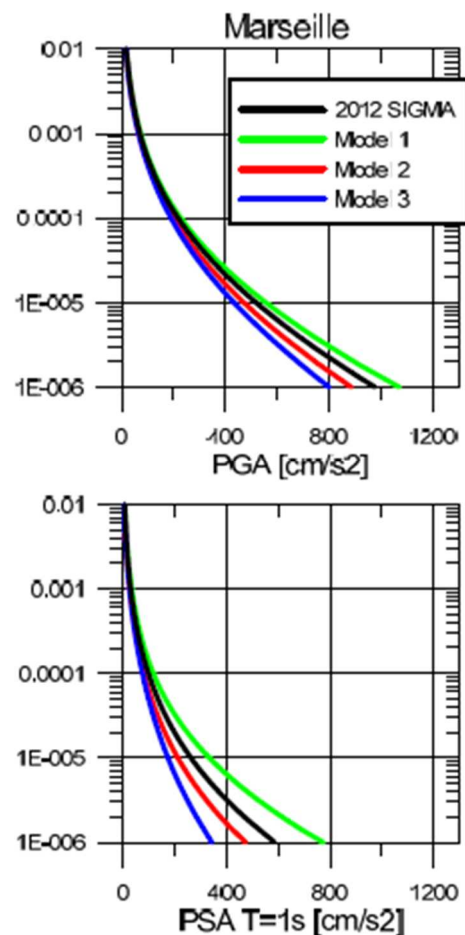


**Figure 3:** Impact of different choices of  $m_{max}$  (sigma study and 3 alternative approaches for  $m_{max}$ ) on the hazard curve (annual probability of exceedance) for PGA and PSA at 1Hz, from Ameri et al (2014).

The justification of the choice of  $m_{max}$  only from physics or simple statistics is not straightforward. Concurrently, recent analyses showed that the maximum magnitude can have a major impact on the hazard curve when high return periods as required for safety analysis of NPP (20 000 years) are considered, see Ameri, 2014. This is illustrated in **Figure 3** where some result of the sensitivity studies conducted in SIGMA project are shown. The hazard curves obtained with  $m_{max}$  determined with different methods and assumptions differ for higher return periods. The 3 models represent the cases where 1) the SHARE values are adopted, 2) the Bayesian updating according to EPRI 1994 is used and 3) an increment and scaling based method using French data. More details can be found in the report by Ameri et al (2014).

The maximum magnitude is generally determined for zones in which seismicity is assumed to be uniform. However, there are only few observations of extreme magnitudes in low to moderate seismicity regions such as France which makes it difficult to assign a reliable number to  $m_{max}$ . The estimation of  $m_{max}$  by means of a Bayesian approach allows for the combination of different sources of information coming from physics, statistics and other available knowledge.

This report addresses the estimation of the maximum magnitude in the truncated GR law by means of a Bayesian approach involving extreme value statistics. We propose a new method, which constitutes an improvement of former developments by EPRI, see Johnston (1994), and further promoted by USNRC (2012). The proposed methodology combines the distribution of extreme values of the truncated GR law with the Bayesian updating approach in order to account for prior information from similar tectonic zones and expert judgment.

## 1. Short literature review

There are essentially three types of approaches that have been pursued in the past to determine the maximum magnitude  $m_{max}$ .

The simplest method is purely empirical and consists of adding an increment (in general 0.5 magnitudes units) to the largest magnitude observed in the zone or region of interest (see e.g. the review in Wheeler 2009). The physical approach consists in considering fault geometry, and length and possibly paleo-seismicity to deduce information on the energy that could be released (see also Zöller & Holschneider, 2016). In addition, deformation rates from geodetic data & long-term tectonic deformation are gaining increased interest for the determination of maximum magnitudes (e.g. Anderson 1979, Main & Burton 1984, Moravos et al 2003, Rong et al 2017, Stevens & Avouac 2017). Eventually, the theory of statistics of extremes has been applied in engineering seismology since the early 'fifties by different authors such as Nordquist, 1945, Epstein & Lomnitz, 1966, Knopoff & Kagan, 1977. The developments concern both the estimation of  $m_{max}$  of the truncated GR distribution and the direct estimation of the tails of the magnitude distribution by the generalized extreme value and Pareto distributions. Burton & Makropoulos, 1985 express the distribution of maximum magnitude by an extreme value distribution of Weibull type which has an upper bound to be estimated. The authors use no prior information so the uncertainty in the maximum magnitude is very large. Pisarenko et al., 2003, 2008, 2014, adopt the more general framework of the generalized extreme value distribution. The theory of extreme value statistics shows that the generalized extreme value distribution is the limit distribution of the maximum, of a series of independent random variables with same distribution under the condition of appropriate normalization. However, the scarcity of data in low seismicity regions can make it difficult to apply the latter methods. On the other hand, it is well known that the maximum likelihood estimator (MLE) of the magnitude used to truncate the GR law is biased (Kijko, 2004, 2012). The maximum likelihood estimate

corresponds to the maximum of the likelihood function which is always equal to the highest observed magnitude  $m_{\max\text{obs}}$  in this case, as illustrated in **Figure 4**. As the number of observed earthquakes and thus the sample size  $n$  increases it becomes more and more likely that  $m_{\max\text{obs}}$  is the true  $m_{\max}$  and the likelihood function gets more and more concentrated around this value. However, when increasing the sample size  $n$ , then the estimator converges to the “true” value but from below. Kijko, 2012 developed a bias corrected maximum likelihood estimator to estimate  $m_{\max}$ . The derivation of the correction term is however based on some simplifying assumptions.

The Bayesian updating approach adopted here allows for the combination of different sources of information, and to overcome the problem of bias of the simple maximum likelihood estimator (EPRI 1994, USNRC 2012). The development of the prior relies on drawing analogies with tectonically comparable regions to increase the dataset for the development of generic distribution that can be updated for particular configurations (EPRI 1994, Ameri et al 2015).

The Bayesian approach for estimation of  $m_{\max}$  has been blamed for producing results that are also biased to low values, see for example in Kijko 2009. The authors however only consider the mode of the posterior (similar to the Maximum Likelihood solution) as the point estimate of  $m_{\max}$  which leads to the bias and does not consider the full posterior density function or its mean. Here we use the full posterior distribution in the application of the Bayesian approach for  $m_{\max}$  estimation, and confirm that the posterior mean, sometimes called the “Bayes estimator” (see e.g. Jaynes 2007) is a better point estimator for  $m_{\max}$ . Moreover, the case studies presented in USNRC (2012) confirm that the Bayesian posterior does not display any significant bias: “Therefore, it is concluded that the application of the Bayesian approach using the full posterior distribution should not lead to biased estimates of  $m_{\max}$ .” Obviously, if the data is scarce, then the posterior distribution is close to the prior such that the latter has a major impact on the estimation. This is why the prior distribution has to be developed with care. Nevertheless, we anticipate that the studies conducted here for French data showed that the available observations drive the estimations and have a significant impact on the estimates.

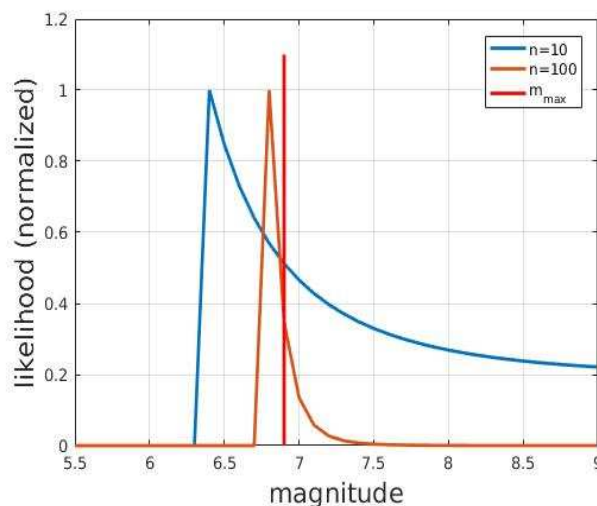


**Figure 4:** Convergence and bias of the MLE for  $m_{\max}$  in the truncated GR law: the figure shows an example of likelihood functions for true  $m_{\max}=6.8$  and considering  $n=10$  and  $n=100$  observations.

Zöller et al (2016) and Holschneider et al (2016) argue that the modeling context of a doubly truncated GR law allows for the inference of the maximum possible magnitude only if unrealistically large catalogs are available. The authors (Zöller et al 2013) suggest replacing it by the maximum expected magnitude on a particular time horizon, for which confidence intervals can be computed from an earthquake catalog

in the framework of Gutenberg–Richter statistics. This proposal can be useful in particular contexts, for example in the framework of a deterministic assessment where a Maximum Considered Earthquake (MCE) has to be defined. It has to be pointed out that the distribution of the maximum magnitude on a time horizon has a fundamentally different meaning from the estimation of the maximum magnitude in the truncated GR law. First, for determining the maximum magnitude in a time horizon in the framework of the GR law, it is still necessary to determine the truncation of the GR law or, else, to work with the untruncated GR law. The latter however leads to very high expected magnitudes for large time horizons such as considered in probabilistic risk assessment in the nuclear sector. Secondly, in contrast to the distribution of the maximum magnitude used to truncate the GR law, the distribution of the maximum magnitude on a time horizon does not represent epistemic uncertainty but aleatory variability (each of the maximum magnitudes could happen to be the maximum value over one such time interval, with different probabilities of occurrence). This has to be taken into account when choosing for example a deterministic design value, such as the 95% non-exceedance value on the time horizon.

Here, we rather show by means of simulated catalogues, that, when assuming the truncated GR distribution for the simulated magnitudes, it is possible obtain a meaningful estimate of  $m_{\max}$  based on available data. The Bayesian updating approach does allow for the combination of evidence from prior information and data (USNRC, 2012) and thus to overcome certain problems raised by Zöller et al. (2014).

## 2. Extreme value distributions

### Generalized extreme value distribution

Extreme value theory is a branch of statistics that deals with the extreme values of probability distributions. Extreme value statistics provide mathematical methods and tools for the law of extremes defined by the tails of probability distributions.

By the extreme value theorem the GEV distribution is the only possible limit distribution of properly normalized maxima of a sequence of independent and identically distributed random variables. It has to be acknowledged that a limit distribution may not exist. Nevertheless, the GEV distribution is often used as an approximation to model the maxima of long sequences of random variables.

Let us consider a sequence of  $n$  random variables  $X_1, X_2, \dots, X_n$  with common CDF  $F(x)$  and the random variable

$$M_n = \max\{X_1, X_2, \dots, X_n\} \quad (2)$$

The CDF of the maxima  $M_n$  of the sequence is then simply expressed as:

$$P(M_n < x) = F(x)^n. \quad (3)$$

However, the function  $F(x)$  is generally not known. Moreover, small errors on the quantity  $F(x)$  can lead to important errors in the product  $F(x)^n$ . An alternative consists in the direct estimation of the quantity  $F(x)^n$ . It can be shown that for large  $n$  and when choosing appropriate normalizing constants  $a_n, b_n$  (see e.g. Coles, 2001) we have:  $P\left(\frac{M_n - b_n}{a_n} < z\right) \rightarrow G(z)$  where

$$G(z) = \exp\left\{-\left[1 + \xi\left(\frac{z-\mu}{\sigma}\right)\right]^{-1/\xi}\right\} \quad (4)$$

represents the family of generalized extreme value distributions (GEV), with parameters  $\mu, \sigma > 0$  and  $\xi$  that have to be determined. The parameters  $\mu$  and  $\sigma$  define localization and scale. The parameter  $\xi$  is



called the “shape parameter” since it determines to which of the three possible families of extreme value distributions the variable belongs.

The three CDF of the GEV family have different domains of attraction. For  $\xi = 0$  the GEV yields the Gumbel distribution. It is unbounded (no lower and upper bound) and is also referred to as the extreme value distribution of type I (GEV I):

$$G^I(z) = \exp\{-\exp\{-(z - \mu)/\sigma\}\}, \quad -\infty \leq z \leq \infty. \quad (5)$$

For  $\xi \neq 0$ , et  $\left\{z: 1 + \xi \left(\frac{z-\mu}{\sigma}\right) > 0\right\}$  we have:

$$G(z) = \exp\left\{-\left[1 + \xi \left(\frac{z-\mu}{\sigma}\right)\right]^{-1/\xi}\right\}. \quad (6)$$

In the other cases:

- If  $\xi > 0$ ,  $G(z)$  yields the Fréchet distribution with a lower bound, it is also known as the extreme value distribution of type II (GEVD II).
- For  $\xi < 0$ ,  $G(z)$  yields the returned Weibull distribution with an upper bound:  $G(z) = 1$  si  $z \geq \mu - \frac{\sigma}{\xi}$  (distribution of the minima), this is called the extreme value distribution of type III (GEVD III).

The typical shapes of the three different distributions are illustrated in **Figure 5** below. The Fréchet (GEVD II) distribution exhibits a thick tail while the Gumbel distribution (GEVD I) has a light tail, the Weibull distribution (GEVD III) has an upper bound. The ordinary Weibull distribution occurs in numerous reliability problems and is obtained by using the variable  $t = \mu - z$  which leads to a strictly positive support for the probability distribution. The exponential and normal distribution have extreme value distributions of type I (this concerns the GR law if it is not truncated by  $m_{\max}$ ).

The extreme value distribution is max-stable, which means that the maximum of a suite of  $k$  maxima  $M_{n,1}, \dots, M_{n,k}$  follows the same distribution as  $M_n$ , under the condition of proper normalization (localization and scale). More precisely, a distribution  $G$  is said max-stable if there exist constants  $a_n, b_n$  such that  $G(a_n z + b_n)^n = G(z)$ .

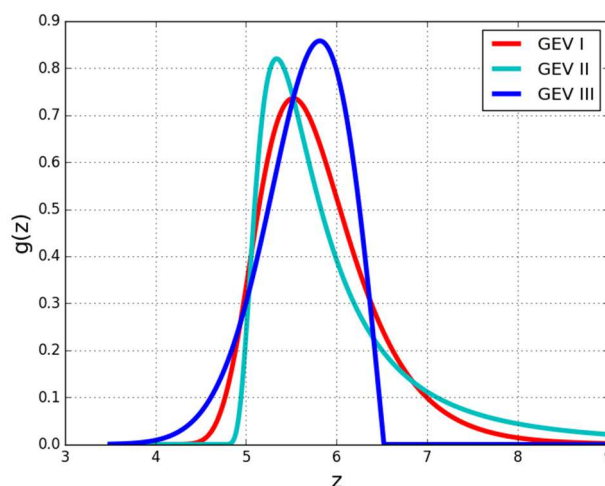


**Figure 5:** Illustration of the three types of extreme value distributions.

The parameters of the generalized extreme value distribution are generally estimated by maximum the likelihood estimator. For a given set of parameters  $\{z_i: 1 + \xi \left(\frac{z_i - \mu}{\sigma}\right) > 0\}, i = 1, \dots, n$ , et  $\xi \neq 0$ , the log-likelihood function reads

$$L(\mathbf{z}_n | \mu, \sigma, \xi) = -n \ln \sigma - (1 + 1/\xi) \sum_{i=1}^n \ln \left[ 1 + \xi \frac{z_i - \mu}{\sigma} \right] - \sum_{i=1}^n \left[ 1 + \xi \frac{z_i - \mu}{\sigma} \right]^{-1/\xi} \quad (7)$$

It is possible to regularize the optimization problem by the introduction of an a priori information on the parameters by a Bayesian approach.

### Generalized Pareto distribution (GPD)

We consider a random variable with cumulative density function (CDF)  $F(x)$ . The CDF of the exceedance of a threshold  $u$  can be expressed as the conditional probability density function (PDF) (e.g. Coles 2001):

$$P(X > u + y | X > u) = \frac{1 - F(u+y)}{1 - F(u)}, y > 0. \quad (8)$$

In general,  $F(x)$  is not known, but it can be approximated by the generalized Pareto distribution. More precisely, for  $u$  sufficiently large, the CDF of  $y = (x - u)$  conditioned on  $X > u$ , can be approached by the Generalized Pareto Distribution (GPD):

$$H(y) = 1 - (1 + \xi y / \tilde{\sigma})^{-1/\xi}, \quad (9)$$

$$\{y: y > 0, (1 + \xi y / \tilde{\sigma}) > 0\}$$

where  $\tilde{\sigma} = \sigma + \xi(u - \mu)$  (with increasing threshold, the distribution tends towards the Pareto law). The parameter  $\xi$  is equal to the one of the generalized extreme value distribution. If  $\xi < 0$ , then the generalized Pareto law is bounded by an upper threshold equal to  $\mu - \frac{\tilde{\sigma}}{\xi}$ .

**Example:** Given the exponential distribution  $F(x) = 1 - e^{-y}$ , one has  $\frac{1 - F(u+y)}{1 - F(u)} = e^{-y}$  for all  $y$ , which corresponds to  $\xi = 0$  and  $\tilde{\sigma} = 1$  in the GPD.

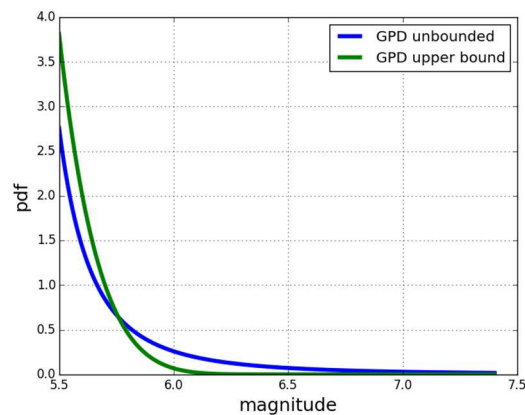


**Figure 6:** Examples of two Pareto laws (unbounded and with upper bound) to represent the tail of a distribution.

## Implication on earthquake recurrence and extreme magnitudes

For earthquake recurrence, this means that if the truncated GR distribution is assumed, then the CDF  $F(x)$  is known (it is indeed a truncated exponential distribution) and the extreme value distributions can be derived analytically. By construction, it is in the domain of attraction of the GEV of type III with an upper bound. More precisely, it is the Weibull distribution with upper bound and  $\xi < 0$ . The upper value of the considered variable ( $x$ ) is given by the relation  $\mu - \frac{\sigma}{\xi}$ . The parameters of the extreme value distribution can be estimated by the maximum likelihood method (Coles, 2001). The most commonly used recurrence model is the GR law assuming Poissonian occurrence of earthquakes. It explicitly excludes aftershocks and more generally triggered events. The model and the associated extreme value distributions are described with more detail in the following section. If no assumption is made on the distribution of the magnitudes, then the estimation of the parameters of the GEV allows for assessing whether the data predicts a bounded distribution and to evaluate the parameters. However, if, as it is currently common practice, a truncated GR model is assumed than the most coherent and robust way is to introduce this information in the  $M_{max}$  parameter estimation as derived in the following sections.

The estimation of  $M_{max}$  by extreme value distributions is illustrated in **Figure 7** to **Figure 9** below. The blue dots are the magnitudes obtained for a simulated catalogue using the GR law with  $b=0.9$ ,  $\lambda=3.75$ ,  $m_{min} = 4.0$  and  $m_{max} = 7.0$ . The details of these models are given in the section below. At this stage, the figures are only shown for illustration.

**Figure 7** shows two examples of sample of extreme magnitudes retained for the GPD approach considering two different thresholds. The threshold is  $M_w = 5.5$  on the left side and  $M_w=6.0$  on the right side. The result depends of course on the particular sample catalogue. The simulations are done for a catalogue of 2018 years and there is considerable variability. **Figure 8** shows another result for  $M_w=6.0$  but this time, there is no exceedance.

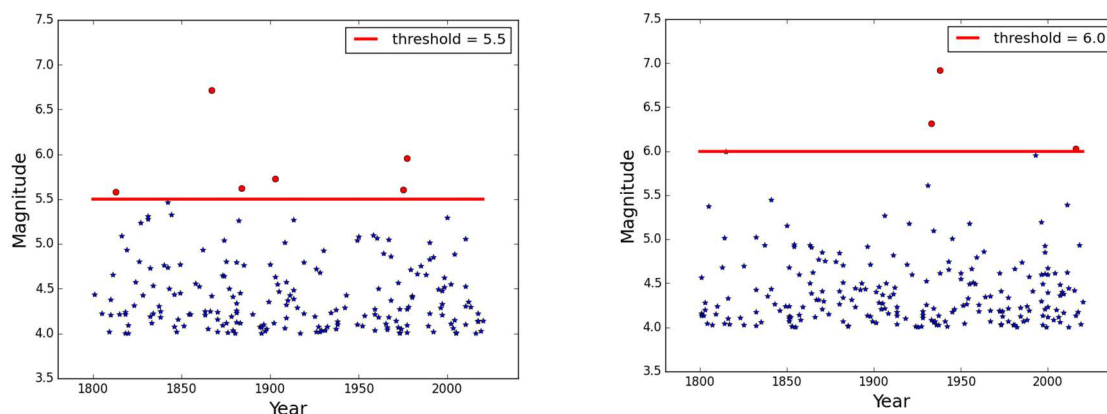


**Figure 7:** Illustration of sample of extreme magnitudes retained for estimation with GPD approach and choosing a threshold of  $M_w=5.5$  (left) and  $M_w= 6.0$  (right). All magnitudes above the threshold (red dots) are retained for statistical analyses.

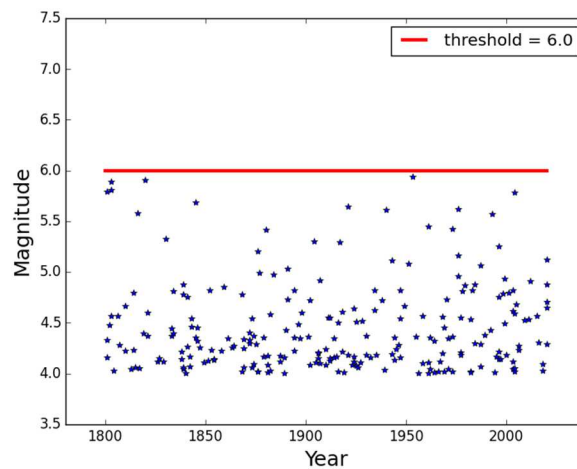


**Figure 8:** Another example sample of extreme magnitudes retained for estimation with GPD approach and choosing a threshold of  $M_w = 6.0$ . There is no magnitude above the threshold.

**Figure 9** shows two examples of sample of extreme magnitudes retained for the GEV approach considering two different choices of time intervals. There is only one time interval and the maximum magnitude on the left side and 10 intervals leading to a sample of 10 extreme magnitudes on the right side. We anticipate here that, when construction the likelihood function for the extreme values (GEV approach) of the GR model, then there is no considerable difference in the result when considering one long interval (duration of catalogue) associated to the maximum observed magnitude as compared to the case where that time interval is partitioned into 10 subintervals and the sample of 10 maximum magnitudes is studied. A similar conclusion is drawn in Zöller & Holschneider (2016).

Lastly, we illustrate, the

- possibility to estimate parameters of the GR law by direct estimation with the extreme value distributions
- convergence of the direct estimation as a function of the duration of the catalogue

The parameters of the GR law are the same as in the former simulations. It has to be pointed out that these values correspond to a high seismicity region. The parameters close to French data (see section 4) were not used for this illustration, because the estimated extreme value distributions were in many cases unbounded. It is also acknowledged that the simulated catalogues do not address the issue of completeness since we consider that the underlying GR distribution is known on the whole magnitude interval.

We construct 1000 simulated catalogues with duration  $T = 2000$ ,  $T = 4000$  years and  $T = 8000$  years, divided respectively into 10, 20 and 40 time intervals of 200 years and we estimate the parameters of the GEV distribution using the maximum likelihood estimator. Again, the simulations have been performed for the high seismicity GR parameters. It is acknowledged here, the considering GR parameters from the French catalogue (low to moderate seismicity) leads in most cases to unbounded GEV distribution.

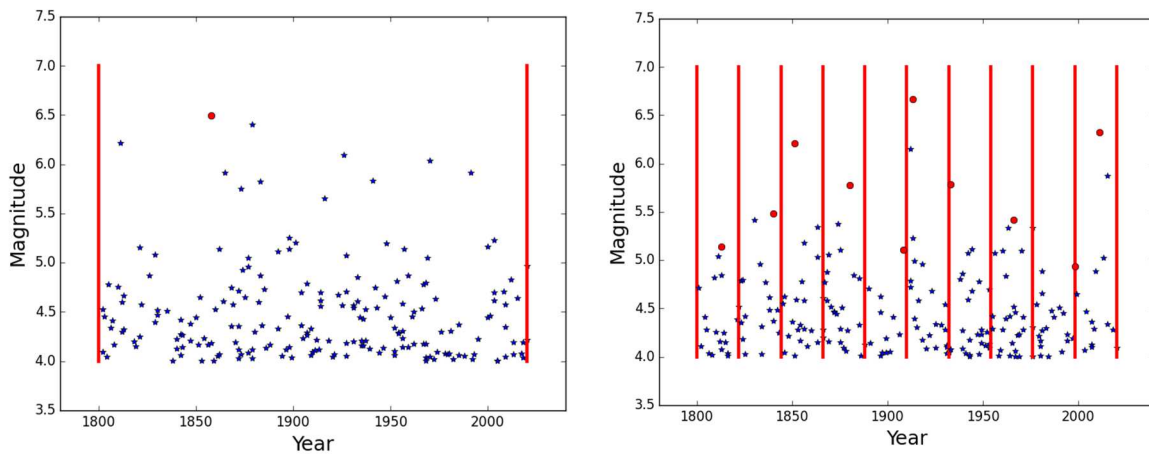


**Figure 9:** Illustration of sample of extreme magnitudes retained for estimation with GEV approach and partitioning the period if observation respectively in only time interval (left) and 10 time intervals of 100 years each (right) where the maxima are retrieved. The maxima of the considered time intervals (red dots) are retained for statistical analyses.

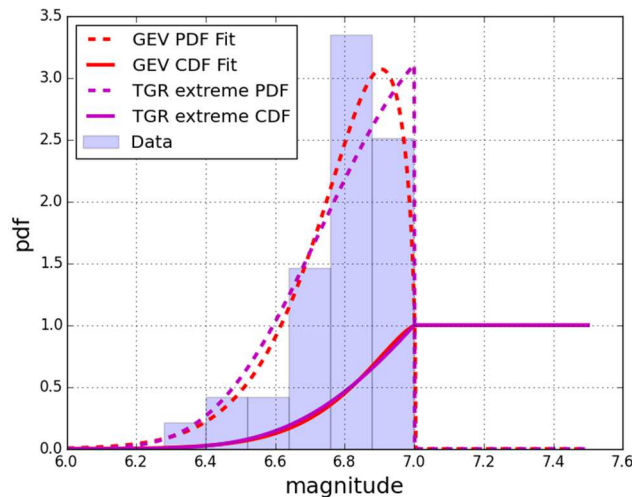


**Figure 10:** Histogram of the sample of 20 extreme magnitudes in the catalogue (Data, 20 time intervals of duration 500 years) and fitted GEV distributions (red) compared to the known analytical extreme value distributions (magenta).

The simulation of a set of 1000 catalogues allows for the estimation of the mean together with its standard deviation (std). Remember that the exact (known underlying) value is here  $m_{max} = 7.0$ . For  $T=8000$  years the std is small which means that a reliable and accurate estimate could be obtained with one catalogue (as would be the case in real life) if it is complete (which is not the case in real life). **Figure 10** shows the histogram of the data (one simulated catalogue) together with the estimated GEV distributions. It can be observed that the empirical distributions are close to the underlying analytical distributions (used for the simulation of the catalogue) for  $T = 8000$  years. For  $T=2000$  years, the statistics were established by disregarding the 3 cases where an unbounded GEV was identified.

The application also highlights that a direct application of the extreme value distribution is not feasible in low to moderate seismicity areas under the assumption of a GR law.

**Table 1:** Mean and std of the sample of posterior means of  $m_{\max}$  determined from 1000 simulated catalogues for different durations T divided into time intervals of 200years.

catalogue	T = 2000 years	T = 4000 years	T = 8000 years
mean $m_{\max}$	6.99	6.99	6.99
std $m_{\max}$	0.36 (3 catalogues lead to unbounded $m_{\max}$ distributions and were discarded)	0.094	0.015

### Poisson model for earthquake recurrence

The occurrence of earthquakes is generally modelled by the Poisson distribution. It is a discrete law that models the number of events over a given time interval.

Given  $\lambda$ , the mean number of occurrences in the time interval, the probability that there are exactly  $k$  occurrences is expressed as

$$p_k(k, t) = \frac{(\lambda t)^k}{k!} e^{-\lambda t}, \quad k = 0, 1, 2, \dots \quad (10)$$

The mean and the standard deviation of the Poisson law are equal  $\lambda$ . The sum of two independent Poissonian random variables still follows the Poisson distribution. It is thus possible to sum the activity of two faults or zones.

In consequence, the probability to have no event between the instants 0 and t can be written as:  $p_k(0, t) = P(T > t) = e^{-\lambda t}$ . This expression allows for deriving the cumulative density function for the time intervals T (we note capital letter to design the random variable and not the particular realization t):

$$F_T(t) = 1 - e^{-\lambda t} \quad (11)$$

where T is the random variable modelling the time between earthquake events. The probability density function of T is obtained by differentiation:

$$f_T(t) = \lambda e^{-\lambda t}, \quad t > 0. \quad (12)$$

The Poisson model thus implies an exponential distribution of the intervals t between two events.

### The Gutenberg-Richter magnitude distribution and associated extreme value distribution

The Gutenberg-Richter (1954) law expresses the annual rate of earthquakes of magnitude M exceeding the value m as:

$$\ln \lambda(M > m) = \alpha - \beta m \quad (13)$$

where  $\alpha$  (global ratio of earthquakes in the zone considered) and  $\beta$  (ratio between earthquakes with small and large amplitude, a larger  $\beta$ -value means that there are more small earthquakes) are constants.<sup>1</sup>

<sup>1</sup> The GR has been initially derived in log10 base. The equations are recalled in appendix 2.

Introducing moreover the smallest considered magnitude  $m_{min}$ , the annual rate of earthquakes with magnitudes larger than  $m$  then reads:

$$\ln \lambda(M > m) = \alpha - \beta(m - m_{min}) \quad (14)$$

For simplicity we note in what follows  $\lambda_m = \lambda(M > m)$  such that  $\lambda_{m_{min}} = e^\alpha$  is the annual rate of earthquakes. The expression above allows for determining the cumulative density function (CDF) of magnitudes larger than  $m_{min}$  with  $\lambda_{m_{min}} = \lambda_0$  as:

$$F_M(m) = \begin{cases} 0, & m \leq m_{min} \\ 1 - e^{-\beta(m-m_{min})}, & m > m_{min} \end{cases}, \quad (15)$$

The probability density function (PDF) of magnitudes then reads:

$$f_M(m) = \begin{cases} 0, & m \leq m_{min} \\ \beta e^{-\beta(m-m_{min})}, & m > m_{min} \end{cases} \quad (16)$$

Introducing the truncation by the upper magnitude  $m_{max}$  we have:

$$F_M(m) = \begin{cases} 0 & m \leq m_{min} \\ \frac{e^{-\beta m_{min}} - e^{-\beta m}}{e^{-\beta m_{min}} - e^{-\beta m_{max}}} & m_{min} < m < m_{max} \\ 1 & m \geq m_{max} \end{cases} \quad (17)$$

and the distribution of magnitudes becomes:

$$f_M(m) = \begin{cases} 0 & m \leq m_{min} \\ \frac{\beta e^{-\beta m}}{e^{-\beta m_{min}} - e^{-\beta m_{max}}} & m_{min} < m < m_{max} \\ 0 & m \geq m_{max} \end{cases} \quad (18)$$

or, for  $m_{min} \leq m \leq m_{max}$ :  $f_M(m) = \frac{\beta e^{-\beta(m-m_{min})}}{1 - e^{-\beta(m_{max}-m_{min})}}$ .

Under the assumption of Poissonian occurrence and adopting the GR law, one can show that the annual maximum magnitudes follow a Gumbel distribution (extreme value distribution of type I). Indeed, the theorem of total probabilities allows writing the probability that all magnitudes, observed over a time horizon  $\tau$ , are less than  $m$  as:

$$\begin{aligned} G(m) &= \sum_{k=0}^{\infty} \frac{(\lambda_0 \tau)^k}{k!} e^{-\lambda_0 \tau} [F_M(m)]^k, \\ &= \exp[-\lambda_0 \tau (1 - F_M(m))] \end{aligned} \quad (19)$$

The above expression is the cumulative density function of maximum magnitudes over the period  $\tau$ , called  $G(m)$ . The corresponding density function reads:

$$g(m) = \frac{dG(m)}{dm} = f_M(m) \lambda_0 \tau \exp[-\lambda_0 \tau (1 - F_M(m))] \quad (20)$$

The GR law without upper truncation yields  $F_M(m) = 1 - \exp[-\beta(m - m_{min})]$  which leads to the following expression for the distribution of maximum magnitudes observed over the period  $\tau$ :

$$G(m) = \exp[-\lambda_0 \tau \exp(-\beta(m - m_{min}))] \quad (21)$$

Relation (21), called also Lomnitz formula (Epstein & Lomnitz 1966) in the literature, represents the extreme value distribution of type I.

Likewise, it is possible to derive the distribution of maxima accounting for the truncation of the GR law by  $m_{max}$  according to equation (10). In this case, we obtain the following expression for  $m_{min} \leq m \leq m_{max}$ :

$$G(m) = \exp \left[ -\lambda_0 \tau \left( \frac{\exp(-\beta m_{max}) - \exp(-\beta m)}{\exp(-\beta m_{max}) - \exp(-\beta m_{min})} \right) \right] \quad (22)$$

In order to simplify the notations, we will write in what follows  $\lambda_0$  for the annual rate of earthquakes with magnitude larger than  $m_{min}$  (instead of  $\lambda_{m_{min}}$ ).

### 3. Estimation of maximum magnitude by means of Bayesian approach using the extreme value distributions

In what follows, we first give a general description of the Bayesian updating approach. We then show different ways to construct the likelihood function based on the extreme value distribution and conclude with the proposed approach. Afterwards, the EPRI Bayesian updating procedure is described and advantages of the new method proposed here are highlighted.

#### Bayesian updating

The Bayes theorem allows us to write the posterior distribution of the maximum magnitude  $m_{max}$ , denoted  $f(m_{max}|obs)$ , as a product of the prior distribution  $f_0(m_{max})$  of  $m_{max}$  and the likelihood:

$$f(m_{max}|obs) = c L(obs|m_{max}) f_0(m_{max}) \quad (23)$$

with an appropriate normalizing constant  $c$ . In this expression, the likelihood function  $L(obs|m_{max})$  expresses the probability to observe the data (obs, here: regional catalogue), given the model parameter  $m_{max}$ . In order to apply the Bayesian updating we have to determine a suitable prior distribution. For the maximum magnitude, the prior distribution is estimated from a greater amount of data coming from regions with similar tectonics and geological configurations (see EPRI). **Figure 11** provides an illustration of the Bayesian updating approach for  $m_{max}$ .

#### Different ways to express the likelihood function based on the distribution of extremes

The data required to construct the likelihood functions is the observed  $m_{maxobs}$  and the duration  $T$  (duration of catalogue). The likelihood functions are defined based on the extreme value distributions for Poissonian occurrences using the equations (19) and (20) derived in the previous section. If the GR law is assumed, then this yields equations (21) and (22). Nevertheless, any other magnitude distribution parameterized by  $m_{max}$  could be used in the likelihood functions developed below.

The first two function (equations (24) and (25) are applicable only if  $m_{maxobs}$  is included in the more recent part of the catalogue, with data available over the time interval  $T$  (for example 1750-2016 for the French catalogue).



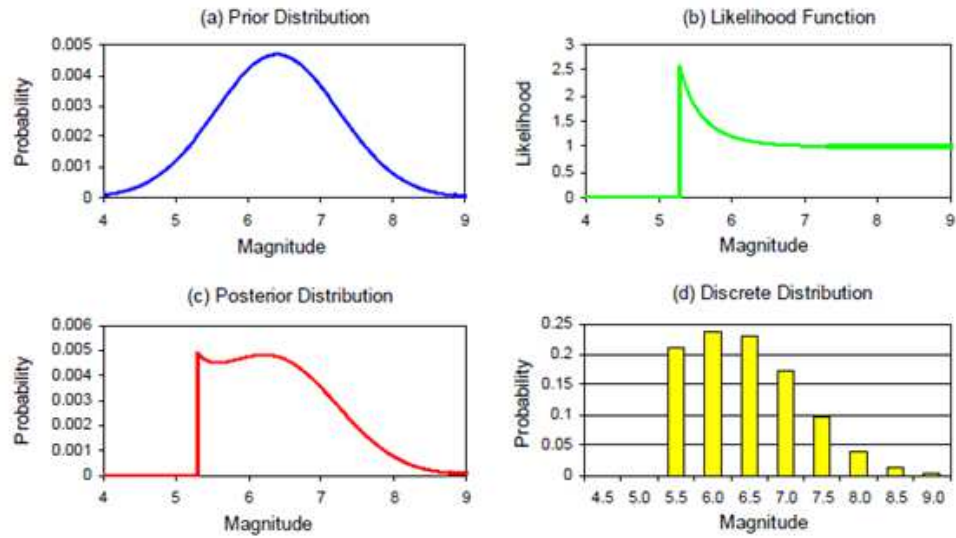


**Figure 11:** Illustration of the Bayesian updating approach applied to the estimation of  $m_{max}$ , figure from PEGASOS.

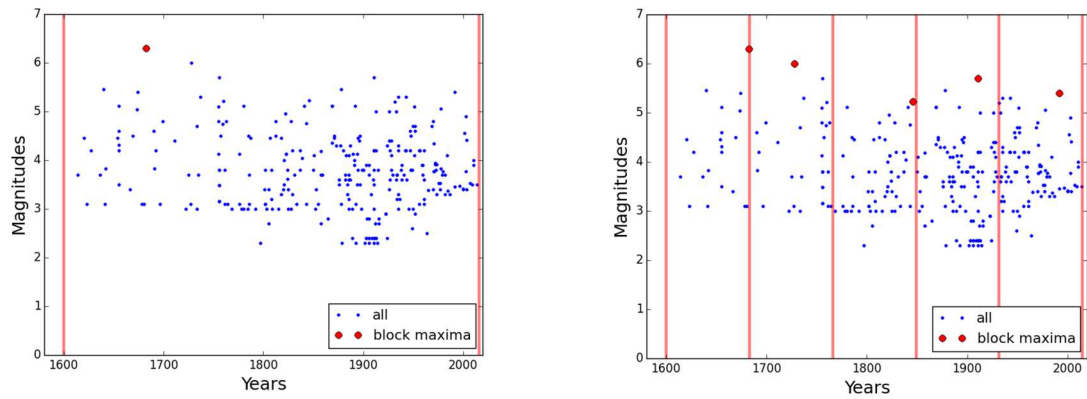


**Figure 12:** Illustration of methods 1a) (left) and 1b) (right) for the construction of the likelihood function.

**1a) Probability to observe  $m_{max_{obs}}$  on interval T (duration of catalogue)**

$$L(obs|m_{max}) = g(m_{max_{obs}}|m_{max}) \quad (24)$$

**1b) Probability to observe set of  $m_{max_{ti}}$  on n time intervals  $\sum_{i=1}^n t_i$**

$$L(obs|m_{max}) = \prod_{t_i} g(m_{max_{ti}}|m_{max}) \quad (25)$$

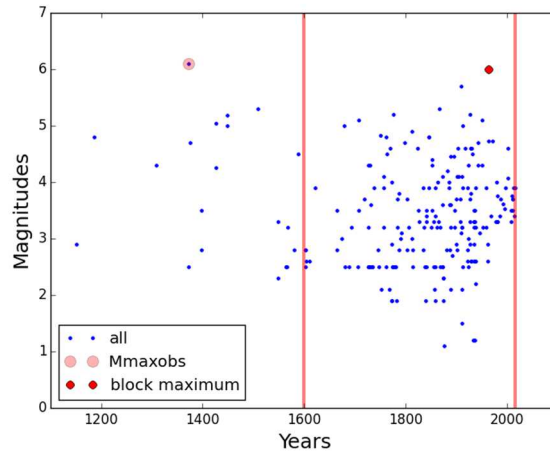


**Figure 13:** Illustration of method 2) for the construction of the likelihood function.  $m_{\max\text{obs}}$  can be outside the completeness interval.

The two cases 1a) and 1b) are illustrated in **Figure 12** for one of the French macrozones introduced in the application section. If the largest magnitude per interval is larger than the completeness magnitude of the considered time interval, then no special consideration of completeness is required to construct this likelihood function for data from a catalogue. The parameters that define the likelihood function are the durations and the values of the maxima over this time interval. Numerical analyses showed that the result is the same of the catalogue is partitioned into equal intervals and the block maxima are used or if the maximum observed earthquake on the whole duration is considered. This is also the conclusion of Zöller & Holschneider (2016). Additional information on past earthquakes is only helpful to constrain the parameters of the seismicity model, for example, the GR parameters  $a$  and  $b$ . This means that the whole duration  $T$  together with  $m_{\max\text{obs}}$  should be chosen (point 1 a) above) to construct the likelihood function since the completeness interval for  $m_{\max\text{obs}}$  is generally rather large. It allows considering the whole (recent part) catalogue without considering the issue of completeness for smaller events, i.e. other than for the justification of the duration  $T(m_{\max\text{obs}})$ .

However, in some cases, the maximum observed earthquake might be outside the interval  $T$ , such as for paléo-earthquakes (see **Figure 13**). In this case, the likelihood function of relation (24) is not applicable, nor the likelihood function given by relation (25). In the latter case, we can still use the constraint that the largest magnitude in the time interval  $T$  is less than  $m_{\max\text{obs}}$ . This is the approach developed in what follows and recommended for further applications.

## 2) Probability that $m < m_{\max\text{obs}}$ on interval $T$ (completeness period for $m_{\max\text{obs}}$ ) – proposed approach

Since  $m_{\max\text{obs}}$  is the largest earthquake observed in the zone, we know that all other earthquakes observed over the period  $T$  of the catalogue are less or equal than this value. We use this information to write the likelihood function as the probability that the largest magnitude in the time interval  $T$  is less than  $m_{\max\text{obs}}$ :

$$L(\text{obs}|m_{\max}) = G(m_{\max\text{obs}}|m_{\max}) \quad (26)$$

Equation (26) is the most general approach and can be applied even if  $m_{\max\text{obs}}$  is outside considered completeness interval  $T$ .

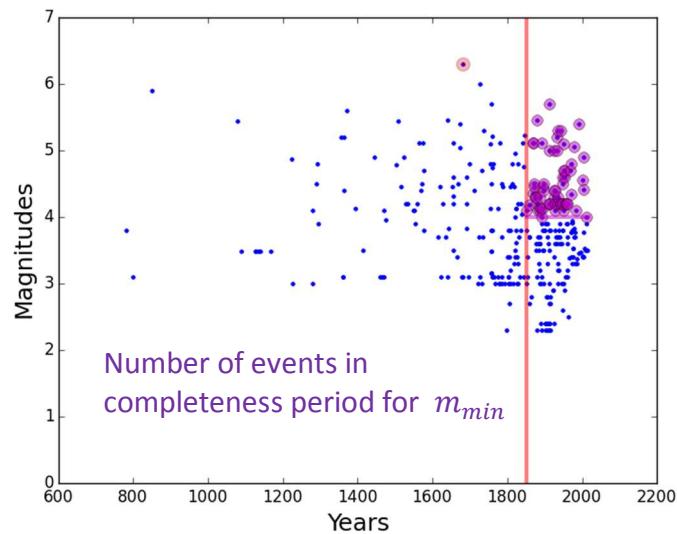


**Figure 14:** Illustration of the EPRI method for the construction of the likelihood function. The number of earthquakes in the completeness period of  $m_{min}$  (magenta dots) are considered. Here,  $m_{maxobs}$  is outside the completeness interval (red dot).

This is illustrated in **Figure 13** for one of the French macrozones introduced in the application section. In the other cases, it provides estimation equivalent to the former relation (24). In consequence, relation (26) will be retained in what follows.

The method does not require any special consideration of completeness periods as long as  $m_{maxobs}$  is in the completeness period of the duration  $T$  and this is generally the case. It can be used if  $m_{maxobs}$  is outside the considered duration  $T(m_{maxobs})$  of the catalogue.

In what follows, we present the EPRI – USNRC approach and highlight the advantages of the new method proposed here.

## EPRI method

### Probability that $m < m_{maxobs}$ over sets of $N$ observations

EPRI (1994) has developed Bayesian updating approach where the likelihood function expresses the probability that all magnitudes in a set of  $N$  observations are less than  $m_{maxobs}$ . This approach is also the recommended USNRC (2012) approach. The likelihood function reads:

$$L(obs|m_{max}) = F_M(m_{maxobs})^N \quad (27)$$

It is noteworthy that this expression (no exceedance for  $N$  observations) is close to the expression used to derive the GEV given by equation (3).

Using the equation (17) for the GR law, we obtain

$$L(obs|m_{max}) = F_M(m_{max|obs})^N =$$

$$c \begin{cases} 0 & m_{max} \leq m_{maxobs} \\ \frac{1}{(e^{-\beta m_{min}} - e^{-\beta m_{max}})^N} & else \end{cases} \quad (28)$$

where the constant  $c$  depends on  $m_{maxobs}$ .

The EPRI Bayesian updating approach uses only the number of observations between  $m_{min}$  and  $m_{maxobs}$  and does not account for duration over which the  $N$  observations are made. This is one major shortcoming. Moreover, the period, over which these earthquakes can be collected and considered in the updating is much smaller than in the new approach proposed here. Indeed, only earthquakes in the completeness periods of  $m_{min}$  can be considered in the count ( $N$ ) and the completeness period of  $m_{min}$  is much smaller than that of  $m_{maxobs}$ . Therefore, the method proposed here leads to smaller confidence intervals and a more accurate estimate. The data used for the EPRI method is illustrated in **Figure 14**.

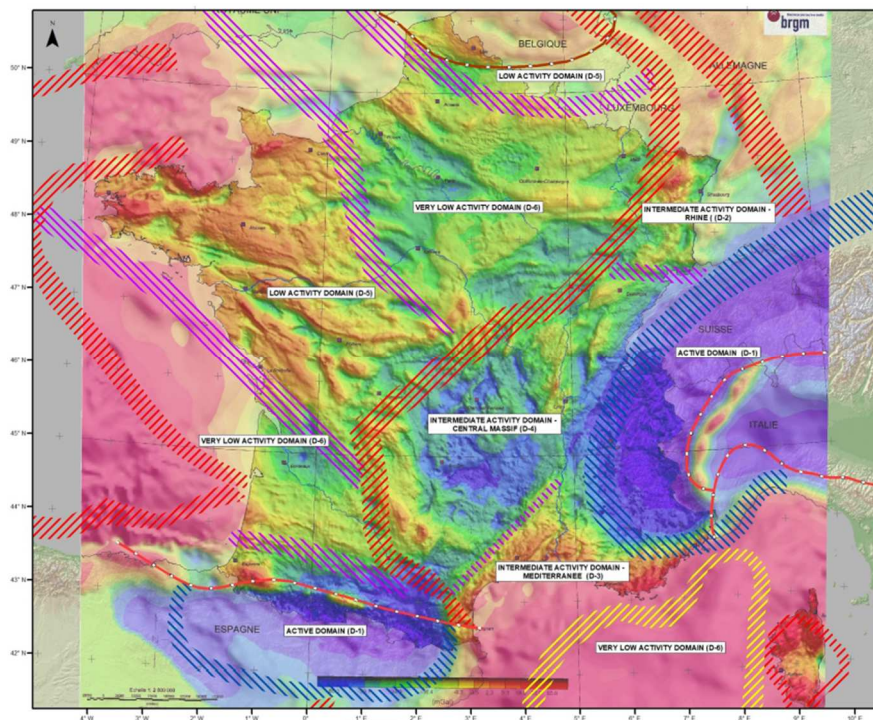


**Figure 15: French Macrozones, GEOTER**

## 4. Application and case studies

We apply the Bayesian updating approach to simulated catalogues and French data.

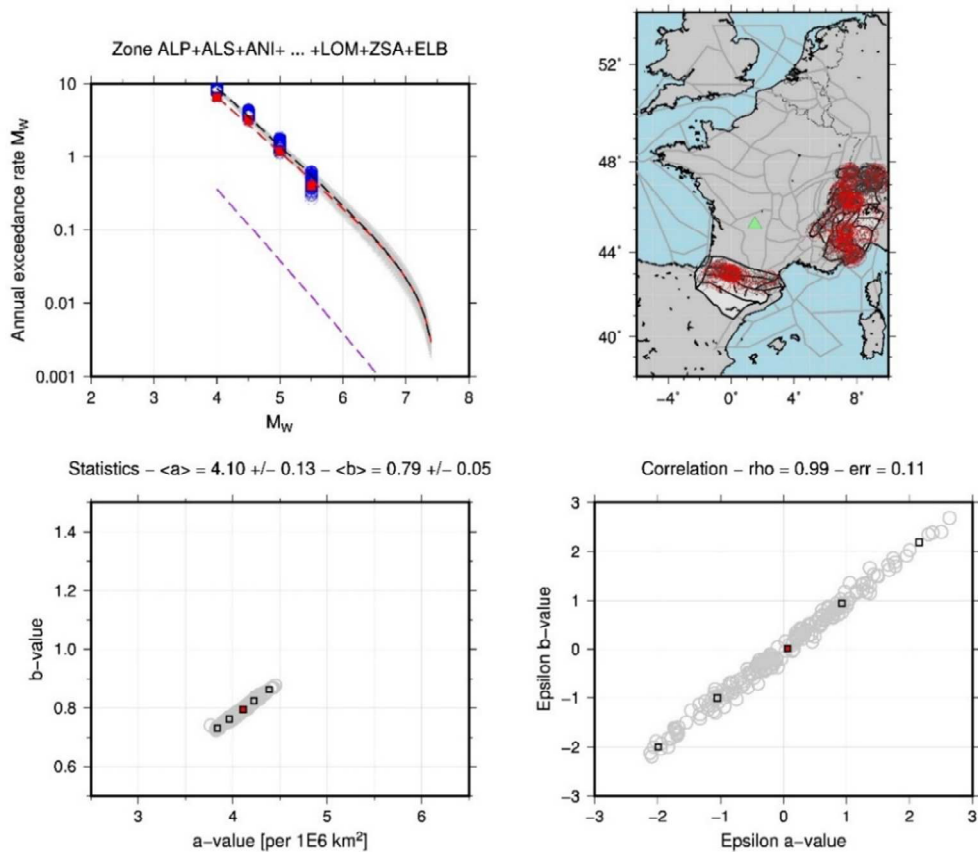


**Figure 16:** Derivation of the GR parameters for macrozone D1, figure from GEOTER.

## French macrozones

The scarcity of larger magnitudes in moderate and low seismicity regions makes it difficult to obtain significant statistics for smaller zones, such as they are often used to derive GR parameters. This why, in the SIGMA project, GEOTER has developed a new division of the French territory that aggregates the smaller zones to 6 macrozones. The macrozonation is shown in **Figure 15**, where Active domains (D 1) are distinguished from the intermediate activity domain - Rhine (D2), the intermediate activity domain - Mediterranean (D3), the intermediate activity domain - Central Massif (D4) and low activity domain (D5), very low activity domain (D6).

In what follows, we will perform analyses for macrozone 1.

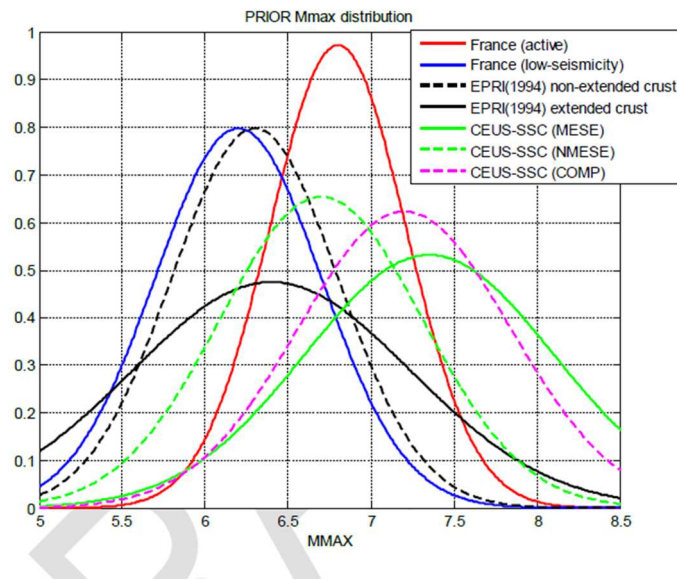


**Figure 17:** Prior distribution determined for France compared to former distributions from EPRI and CEUS, figure from Ameri et al (2015).

### Zone 1

The macrozone 1 comprises the French mountainous domains. It is the zone with the highest seismicity. We use the prior distribution for zone D1 developed by Ameri et al (2015) with the following characteristics:

- Truncated normal distribution
- mean  $M_w=6.8$ , sigma  $M_w = 0.4$
- max  $M_w = 7.5$ , min  $M_w = 5.5$

The GR parameters derived by GEOTER in the SIGMA project for the macrozone D1 are shown in **Figure 16**. The parameters were derived for magnitudes larger than  $m_{min} = 4,5$ . The largest observed magnitude in zone D1 is  $m_{maxobs} = 6,7$ , which occurred within the completeness period T considered (see **Figure 18**).

### Prior distribution

**Figure 17** shows possible candidates for prior distributions. These distributions have been estimated from a greater amount of data coming from regions with similar tectonics and geological configurations (see EPRI 1994, Ameri 2015).

The prior distributions developed by EPRI and others are assumed to be Gaussian without upper or lower truncation. Such a model is not in agreement with physics nor with expert judgment. In order to address this issue, there are two possibilities:

- Define an upper and lower magnitude to truncate the Gaussian prior distribution
- Choose another distribution with a more gradual tail or with explicit upper/lower bounds

In what follows, we have chosen to retain the Gaussian distribution developed by Ameri et al (2015) for France. As proposed in USNRC, a bias correction was applied when developing the prior distribution

from data. The bias correction is based on the assumption that the size distribution of earthquakes in a source region corresponds to a truncated exponential distribution between a specified minimum magnitude and the maximum magnitude for the region (USNRC) and the number of data is corrected for completeness. More details can be found in Ameri et al 2016. We will compare results for the initial Gaussian and the truncated Gaussian prior distribution.

### Analyses conducted with simulated catalogues

The application of the methodology to simulated catalogues allows for an assessment of the accuracy and the convergence of the estimation for given periods of observation. For the simulated catalogues, we chose values for the GR parameters that are close to those of the French macrozone D1 described in the following section. The parameters assumed for the truncated GR law parameters used to simulate the catalogues are:  $m_{\min} = 4.5$ ,  $b = 0.79$ ,  $\lambda_0 = 0.8$ . The  $m_{\max}$  value depends on the study cases. The prior distribution is the one described above for zone D1. We furthermore compare the results to the case where a lognormal prior or a Gaussian prior without truncation is considered. When uncertainty is considered, then a Gaussian error term with a standard deviation of 0.1 is added to the simulated magnitudes. This is a very small value that might not be adequate for the more ancient parts of the catalogue. A more realistic scenario for magnitude uncertainty, depending on the date of the events, will be considered later on. The likelihood function is constructed by means of the distribution of extremes of the truncated GR law using the proposed method given by equation (26). The following two series of studies are conducted:

- 1) We assess the accuracy of the estimations for different values of  $m_{\max}$ . Since, in contrast to the observed earthquake data, the  $m_{\max}$  value is known for the simulated catalogues, we can compare  $m_{\max}$  estimated as the mean of the posterior density function to the “true” value, where the accuracy is formally the difference between the two. Independently, the precision is determined by Bayesian Intervals on the posterior distribution, or estimated from metrics such as the standard deviation in the mean. We consider maximum magnitudes in the range  $M_w = 6.0$  to  $M_w = 7.2$ . To assess the variability, we compute 1000 catalogues for each study case considering  $T = 266$  years.
- 2) We analyze the convergence of the estimations by increasing the period of observation to  $T = 500$  years and  $T = 1000$  years. To assess the variability, we compute 1000 catalogues for each study case with  $m_{\max} = 6.5$ . and  $m_{\max} = 7.0$ .

**Figure 18** below shows the histogram for an example catalogue. The figure shows the histogram of the magnitudes together with the truncated GR target distribution as defined above and for  $m_{\max} = 7.0$  and  $T = 250$  years. **Figure 19** shows the likelihood functions for that same example with  $m_{\max} = 7.0$ . **Figure 20** shows the different priors together with the posterior distribution of  $m_{\max}$ .

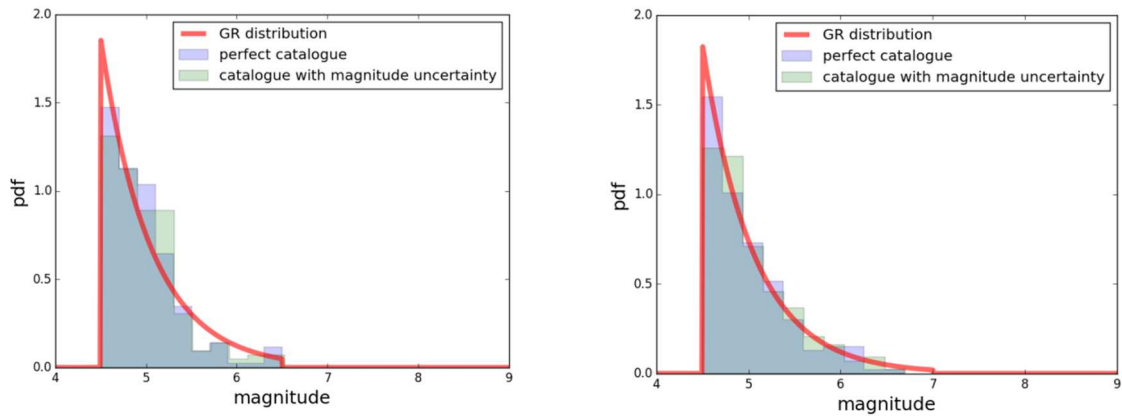


**Figure 18:** Histogram of magnitudes in a simulated catalogue and comparison to truncated GR target distribution with and without consideration of magnitude uncertainty for  $m_{\max} = 6.5$  (left) and  $m_{\max} = 7.0$  (right).

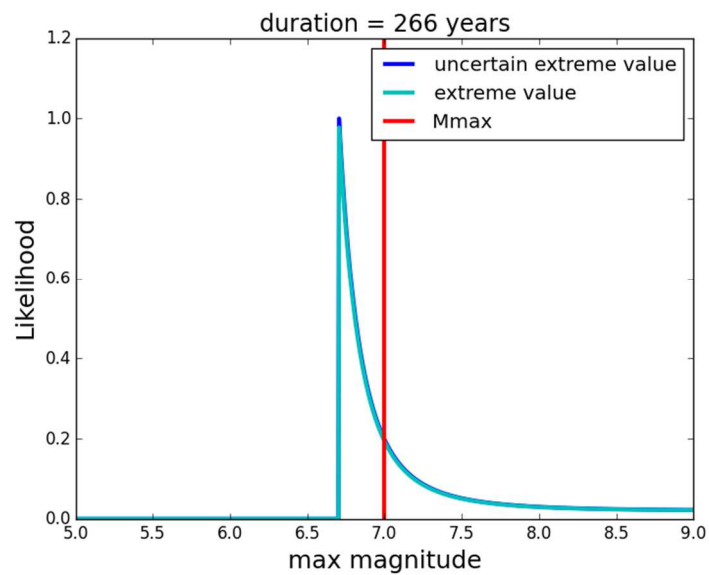


**Figure 19:** Likelihood functions for the case with and without considering uncertainty of magnitudes (example catalogue) and true  $m_{\max}$  used to simulate the catalogues (red).



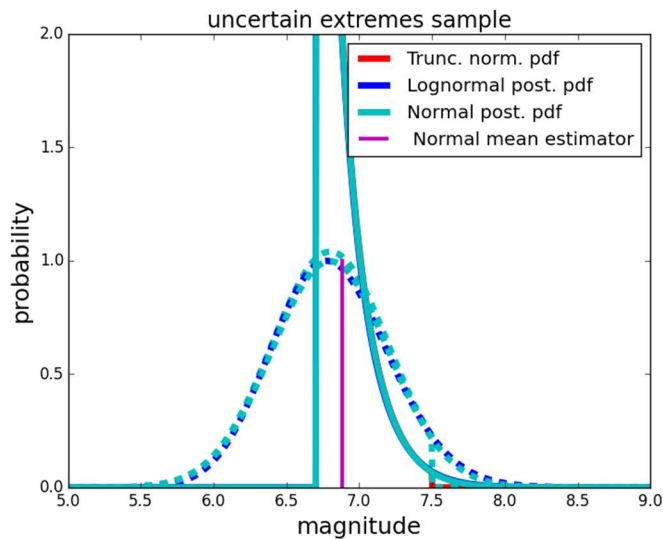


**Figure 20:** Comparison of the posterior distributions (solid lines) for different priors (dotted lines). The posterior distributions are nearly superposed. The Bayes estimator is here the posterior mean (magenta) for the normal prior.

### Study case 1)

All results have been obtained for  $T = 266$  years of observation and a sample of 1000 simulated catalogues. We assume the underlying frequency-magnitude distribution is known, and do not account for this potential source of uncertainty at this stage of the investigation. **Table 2** to **Table 5** show the estimated posterior mean and its std for true  $m_{\max}$  values increasing from  $M_w = 6.0$  to  $M_w = 7.2$ .

**Table 2** Estimated mean and std for true  $m_{\max} = 6.0$  and considering the 3 different priors.

prior	Trunc. normal	lognormal	normal
mean	6.02	6.02	6.02
std	0.04	0.04	0.04

no uncertainty

prior	Trunc. normal	lognormal	normal
mean	6.11	6.11	6.11
std	0.10	0.10	0.10

with magnitude uncertainty

**Table 3** Estimated mean and std for true  $m_{\max} = 6.5$  and considering the 3 different priors.

prior	Trunc. normal	lognormal	normal
mean	6.57	6.56	6.56
std	0.09	0.09	0.10

no uncertainty

prior	Trunc. normal	lognormal	normal
mean	6.61	6.62	6.62
std	0.12	0.13	0.13

with magnitude uncertainty

**Table 4** Estimated mean and std for true  $m_{max} = 7.0$  and considering the 3 different priors.

prior	Trunc. normal	lognormal	normal
mean	6.99	7.00	7.00
std	0.14	0.15	0.15

no uncertainty

prior	Trunc. normal	lognormal	normal
mean	7.01	7.03	7.03
std	0.16	0.17	0.17

with magnitude uncertainty

**Table 5** Estimated mean and std for true  $m_{max} = 7.2$  and considering the 3 different priors.

prior	Trunc. normal	lognormal	normal
mean	7.10	7.13	7.13
std	0.16	0.18	0.18

no uncertainty

prior	Trunc. normal	lognormal	normal
mean	7.12	7.16	7.15
std	0.17	0.19	0.19

with magnitude uncertainty

The analyses show that the Bayesian updating provides good results in the range of magnitudes likely to be the true maximum value for the French context and for observation periods available. Note that in the application to the French catalogue presents in the following section, the considered duration is actually around 270 years, while the results here are given for  $T = 250$  years. The particular choice of the prior distribution (among Gaussian, lognormal and truncated Gaussian alternates) does not have a significant impact on the result in this case. In particular, the estimations of the posterior mean computed with the Gaussian and the truncated Gaussian priors are very close. This is because the data has a major impact on the posterior. The close agreement of the posterior mean with the known  $m_{max}$  within the stated precision implies it is a quite robust estimate, consistent with the results of Jaynes 2007.

### Study case 2)

We increase the period of observation. Note that in the application to the French catalogue presents in the following section, the considered duration is 266 years. The reference results for  $T = 266$  years are given in **Table 3** above. **Table 6** and **Table 7** show the results for  $T = 500$  years and  $T = 1000$  years, respectively.

Considering uncertainty in the magnitude estimates essentially increases the standard deviation of the estimate and thus the error. It also increases the estimated mean, which indicates a (conservative) bias from above. However, the estimates remain sufficiently accurate in both cases.

**Table 6:** Estimated mean and std for true  $m_{max} = 6.5$ ,  $T = 500$  years.

prior	Trunc. normal	lognormal	normal
mean	6.52	6.52	6.52
std	0.05	0.05	0.05

no uncertainty

prior	Trunc. normal	lognormal	normal
mean	6.59	6.59	6.59
std	0.10	0.10	0.10

magnitude uncertainty

**Table 7:** Estimated mean and std for true  $m_{\max} = 6.5$ ,  $T = 1000$  years.

prior	Trunc. normal	lognormal	normal
mean	6.50	6.50	6.50
std	0.02	0.02	0.02

no uncertainty

prior	Trunc. normal	lognormal	normal
mean	6.60	6.60	6.60
std	0.07	0.08	0.07

magnitude uncertainty

**Table 8:** Estimated mean and std for true  $m_{\max} = 7.0$ ,  $T = 500$  years.

prior	Trunc. normal	lognormal	normal
mean	7.00	7.01	7.01
std	0.10	0.11	0.11

no uncertainty

prior	Trunc. normal	lognormal	normal
mean	7.04	7.05	7.05
std	0.13	0.14	0.14

with magnitude uncertainty

**Table 9:** Estimated mean and std for true  $m_{\max} = 7.0$ ,  $T = 1000$  years.

prior	Trunc. normal	lognormal	normal
mean	6.98	7.01	7.01
std	0.06	0.06	0.06

no uncertainty

prior	Trunc. normal	lognormal	normal
mean	7.07	7.07	7.07
std	0.10	0.10	0.10

with magnitude uncertainty

The results show that the Bayesian updating provides an accurate estimate of the maximum magnitude for observation periods available in France, again assuming the underlying frequency magnitude distribution is known. The estimates converge towards the true value if  $T$  is increased and if there is no uncertainty in the magnitudes. For  $T=1000$  years (**Table 7**), the variability of the estimate is negligible ( $\text{std} < 0.03$ ) and the estimated mean is equal to the true value ( $m_{\max} = 6.5$ ). If uncertainty relative to the magnitudes of the catalogue is considered, then there is a bias and the estimated maximum magnitude remains larger than the true value. The error (expressed here by the standard deviation) always decreases when the period of observation is increased.

Finally, we check convergence to the exact value for other maximum magnitudes for  $m_{\max} = 7.0$ . The results are given in **Table 8** for  $T = 500$  years and in **Table 9** for  $T = 1000$  years. The results confirm the previous analyses.

### Accounting for observation period dependent magnitude uncertainty

The magnitude uncertainty assumed for the historical (not experimental) part of the simulated catalogue should be higher than 0.1 in a real case. The value of 0.1 is the std for magnitude uncertainty given in the experimental ground motion database RESORCE for French events, and is an absolute minimum for estimates from historical data, which may change with time. Accordingly, we introduced a Gaussian error term with period of observation dependent std, and considered a moderate uncertainty scenario

and a high uncertainty scenario. The period of observation dependent std of the magnitude uncertainty are shown in **Table 10** for the two cases.

**Table 11** shows the estimated  $m_{max}$  for different true  $m_{max}$  values considering magnitude uncertainty and assuming a normal prior distribution. The simulations show that magnitude uncertainty leads to a systematic overestimation of  $m_{max}$ . The latter increases if the magnitude uncertainty increases. The overestimation of  $m_{max}$  is due to the fact that the observed  $m_{maxobs}$  is generally higher than the “true”  $m_{maxobs}$  when magnitude uncertainty is included. This leads to a bias in the estimations.

This issue can be analyzed with the simulated catalogues by introducing the magnitude uncertainty and by comparing the observed  $m_{maxobs}$  to the true  $m_{maxobs}$  (without magnitude uncertainty). The numerical analyses showed that the relative bias, that is the observed  $m_{maxobs}/true\ m_{maxobs}$ , does not change considerably for different true  $m_{max}$  values but it does depend on the degree of magnitude uncertainty. The bias becomes more significant when the magnitude uncertainty increases. The simulation shows a bias (observed  $m_{maxobs}/true\ m_{maxobs}$ ) of 2.5% for the moderate uncertainty scenario while it becomes 4.5% for the high uncertainty scenario.

An illustration of the origin of the bias is given in **Figure 21** (produced with the moderate magnitude uncertainty scenario). Obviously, without considering magnitude uncertainty, the  $m_{maxobs}$  value cannot exceed the true  $m_{max}$ , which equals 7.0 in this example. However, the observed  $m_{maxobs}$  can be larger than the true  $m_{max}$  within its stated error. Moreover, when the true  $m_{maxobs}$  value is underestimated due to uncertainty this does not mean that  $m_{maxobs}$  is underestimated by that same amount because the second largest magnitude might be larger and then be considered as  $m_{maxobs}$ . This is why, when considering higher magnitude uncertainty, then the observed  $m_{maxobs}$  is generally higher than the true  $m_{maxobs}$  which can lead to a considerable overestimation of  $m_{max}$ . This effect is negligible for very small magnitude uncertainty, such as for example when considering a std of 0.1 as in the first analyses.

The impact of the bias in the observed vs the true  $m_{maxobs}$  is illustrated by the results in **Table 11** where the estimated  $m_{max}$  for the three cases: simulated catalogue without magnitude uncertainty, simulated catalogue with period dependent magnitude uncertainty as explained above. The results highlight that both the magnitude uncertainty and the bias in the observed  $m_{maxobs}$  have to be accounted for when estimating  $m_{max}$ .

**Table 10** Std of the Gaussian distribution assumed for modelling magnitude uncertainty and induced bias in the observed  $m_{maxobs}$  value.

	<1900	<1950	<1975	today
<b>moderate</b>	0.35	0.25	0.2	0.1
<b>high</b>	0.5	0.35	0.25	0.1

**Table 11** Estimated  $m_{max}$  for a true  $m_{max} = 7.0$  with and without bias correction. The table shows the statistics for 1000 simulated catalogues of duration  $T=250$  years considering the moderate and high magnitude uncertainty scenarios.

	No uncertainty	Uncertainty	
		moderate	high
<b>mean</b>	6.99	7.14	7.28
<b>std</b>	0.15	0.24	0.30

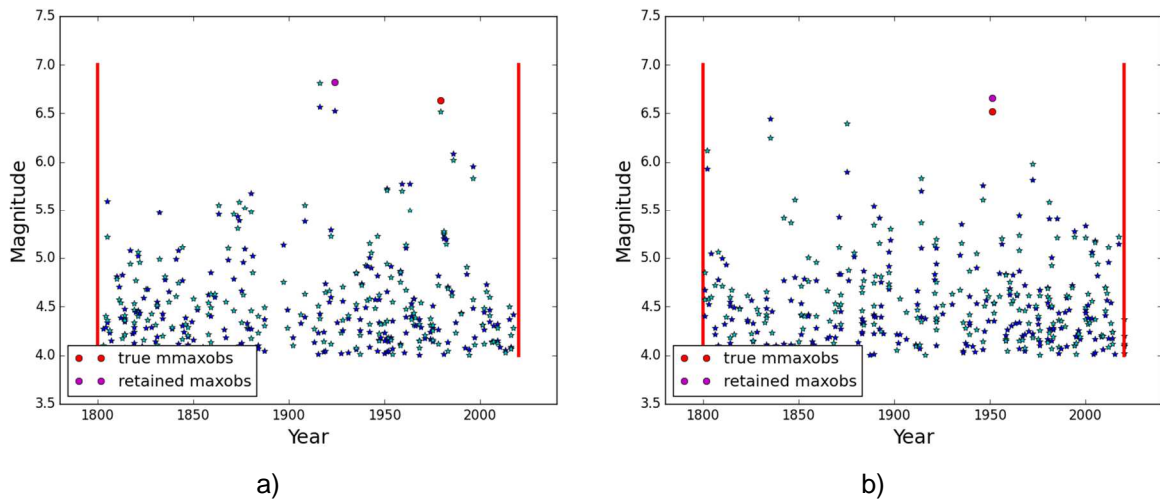


**Figure 21:** Illustration of the case where the a) true  $m_{maxobs}$  and the observed  $m_{maxobs}$  do not belong to the same event and b) where they do

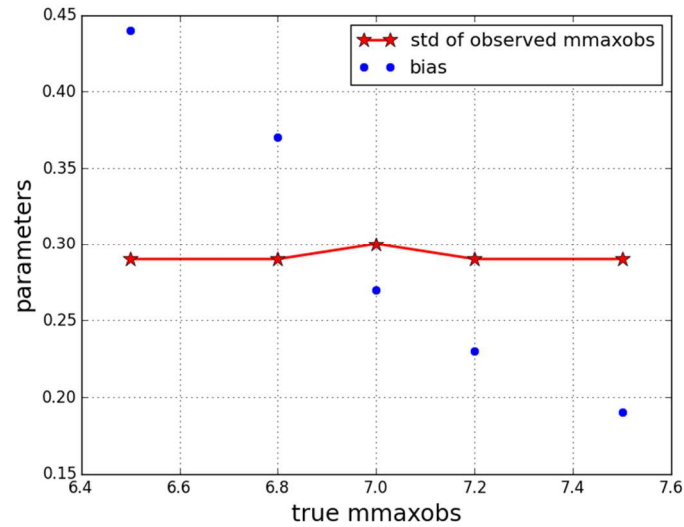


**Figure 22:** Mean and std of the difference between the observed  $m_{maxobs}$  and the true  $m_{maxobs}$  estimated from 1000 catalogues.

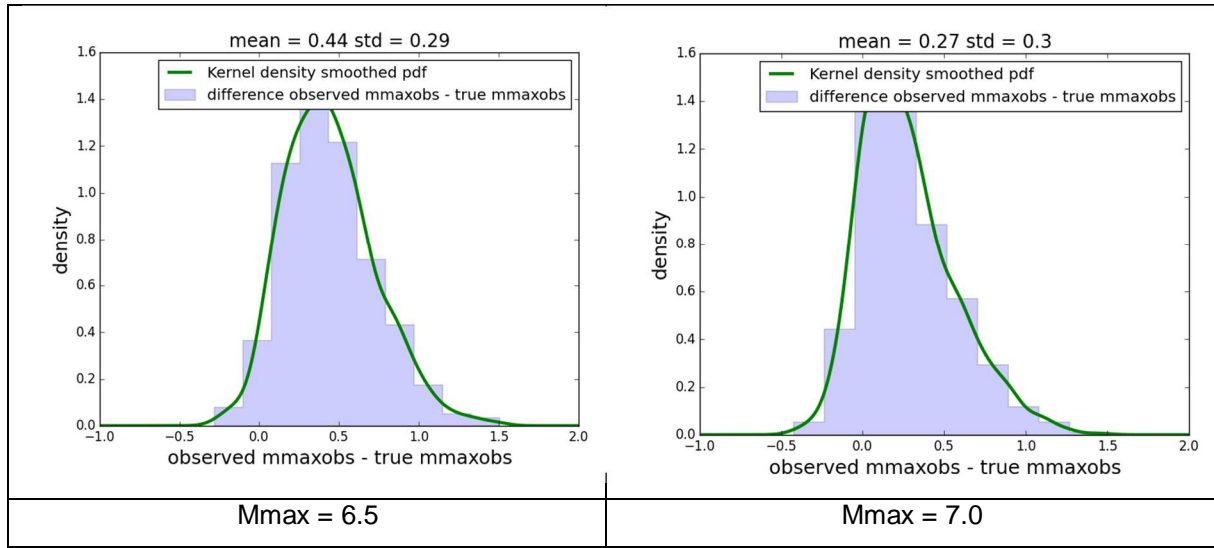


**Figure 23:** Distribution of the difference between the observed  $m_{\max\text{obs}}$  and the true  $m_{\max\text{obs}}$  estimated from 1000 catalogues for the GR parameters of zone D1 and considering different values of  $m_{\max}$ .

In order to fully account for the uncertainty in the observed  $m_{\max\text{obs}}$ , we develop the distribution of the difference between the observed and the true  $m_{\max\text{obs}}$ . For this purpose, the high uncertainty scenario of **Table 10** is adopted. The mean and std of the distribution is evaluated from 1000 simulated catalogues. The results for the GR parameters introduced above (French macrozone D1) and considering different values of true  $m_{\max}$  (not known) are shown in **Figure 22**. It turns out that the standard deviation is around 0.3 and does not depend on the value of  $m_{\max}$  while the mean of the difference between the observed  $m_{\max\text{obs}}$  and the true  $m_{\max\text{obs}}$ , that is the bias, depends on the true  $m_{\max}$ . **Figure 23** shows the detailed results (histogram, smoothed distribution and statistics) for the two cases  $m_{\max}=6.5$  and  $m_{\max} = 7.0$ .

Finally, we analyze the impact of parameter uncertainties on the Bayesian updating procedure. We can consider uncertainty related to the recurrence parameters  $a$ ,  $b$ , the completeness  $T$  and  $m_{\max\text{obs}}$ .

**Figure 16** (the two bottom figures) give the standard deviations and correlation coefficients determined by GEOTER for the GR law of zone D1. In agreement with these results we use a bivariate Gaussian distribution to express the joint law  $f(a, b)$  of the two GR parameters. The correlation coefficient determined by GEOTER is  $\rho=0.99$  which means a « nearly perfectly correlation » of the two parameters. In the light of these results, we assume perfect correlation.

The two perfectly correlated Gaussian random variables  $\beta$  and  $\log_{10}\lambda_0$  are then expressed as:

$$\beta = \ln(10) \bar{b} + \ln(10) \sigma_b \varepsilon \quad (29)$$

$$\begin{aligned} \log_{10}\lambda_0 &= \bar{a} + \sigma_a \varepsilon - m_{\min}(\bar{b} + \sigma_b \varepsilon) \\ &= \bar{a} + m_{\min} \bar{b} + (\sigma_a + m_{\min} \sigma_b) \varepsilon \end{aligned} \quad (30)$$

Where  $\bar{b}$  is the mean estimate of  $b$  and  $\sigma_b$  is the standard deviation and  $\bar{a}$  is the mean estimate of  $a$  and  $\sigma_a$  the standard deviation (all values from **Figure 16**). We adopt a Gaussian distribution for the uncertainty related to  $m_{\max\text{obs}}$  with mean and std according to the results of **Figure 22**.

We evaluate the marginal posterior distribution by integrating the parameter uncertainty in the likelihood function as:

$$\bar{f}(m_{max}|obs) = c \int L(obs|m_{max}, \beta, \lambda_0) f_0(m_{max}) f(\beta, \lambda_0, m_{maxobs}) f(T) d\beta d\lambda_0 \quad (31)$$

$$dm_{maxobs} dT$$

$$L(obs|m_{max}, \beta, \lambda_0) = \exp \left[ -\lambda_0 T \left( \frac{\exp(-\beta m_{max}) - \exp(-\beta m_{maxobs})}{\exp(-\beta m_{max}) - \exp(-\beta m_{min})} \right) \right]$$

The results with and without considering uncertainty are shown in **Table 12**. In particular, we compare the ideal case where the magnitudes in the catalogue are perfectly known to the case where the magnitudes in the catalogue are not perfectly known. In the latter case, **Table 12** shows that the introduction of the uncertainty on the parameters and, in particular on  $m_{maxobs}$ , allows us to improve the estimations (last column of **Table 12**). The posterior mean is close to the true  $m_{max}$  and the std of the estimations (over 1000 catalogues) decreases from 0.28 to 0.16 which is close to the lowest possible value obtained with the perfect data.

**Table 12** Estimated  $m_{max}$  for a true  $m_{max} = 7.0$  with and without improved likelihood function. The table shows the statistics for 1000 simulated catalogues considering the moderate and high magnitude uncertainty scenarios.

	No uncertainty	Catalogue with magnitude uncertainty only	Catalogue with magnitude uncertainty and improved likelihood function
mean	6.99	7.26	7.02
std	0.15	0.28	0.16

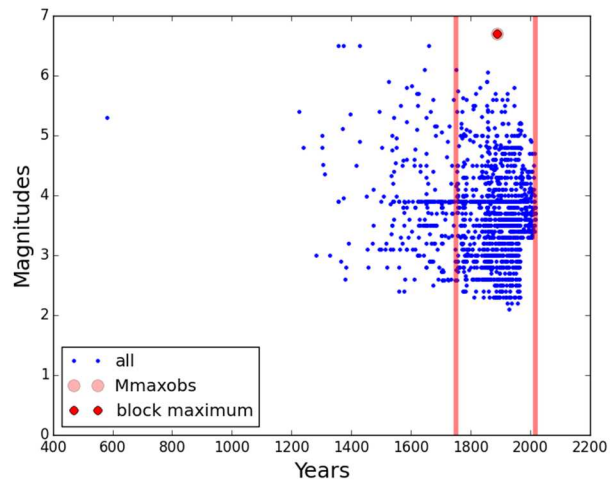
It has to be pointed out that the issue of magnitude uncertainty is unavoidable, and not specific to the new approach presented here (using the likelihood function of equation (26)) but it also needs to be accounted for in the EPRI updating procedure as well as in any other method where a set of extreme magnitudes is considered. In the latter cases, not only the uncertainty of the largest observed magnitude but the uncertainty of the set of magnitudes has to be accounted for according to their occurrence time.

In what follows, we apply the EPRI and the new Bayesian updating approach to French data from catalogue FCAT17 without considering significant magnitude uncertainty. The issue of larger magnitude uncertainty is then addressed in a dedicated analysis.

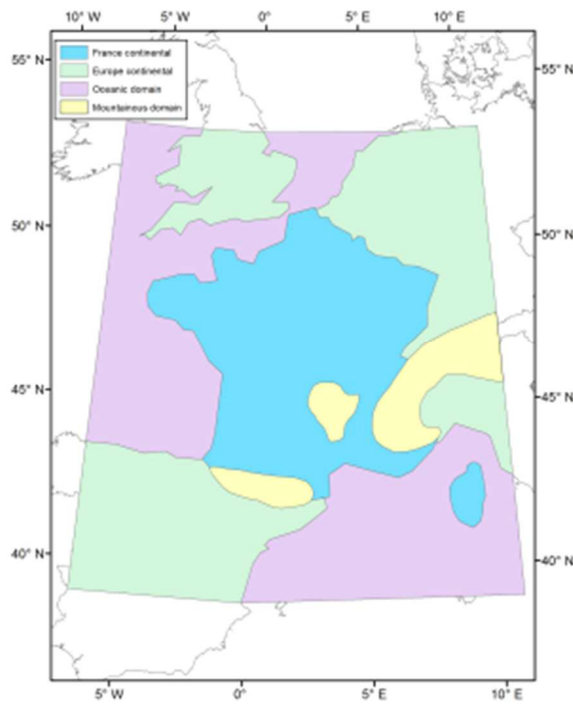
### Analyses with data from FCAT17 catalogue

The French catalogue Fcat14 is used (Manchuel et al., 2017). The data available for macrozone D1 is shown in the **Figure 21** below. The largest observed magnitude in the zone D1 is  $m_{maxobs} = 6.7$ . The largest event occurred on February 23th in 1887 and is within the completeness period as illustrated in **Figure 24**. The GR parameters determined by GEOTER are  $b = 0.79$  and  $a = 4.1$ . (see **Figure 16**), for  $m_{min} = 4.5$ . The completeness periods have been derived previously for mountainous domains in France, see **Figure 25** and **Table 13**. The completeness time period assumed here for  $m_{maxobs}$  starts in the year 1750. For the EPRI method,  $N = 137$  earthquakes have been retained (CEIDRE-TEGG 2017). The truncated Gaussian distribution is chosen as a prior distribution with the parameters developed for the macrozone D1 (Ameri et al 2015) and reported above.

I. Zentner - Bayesian estimation of the maximum magnitude  $M_{max}$  based on the statistics of extremes -



**Figure 24:** Earthquakes contained in the catalogue corresponding to zone D1.

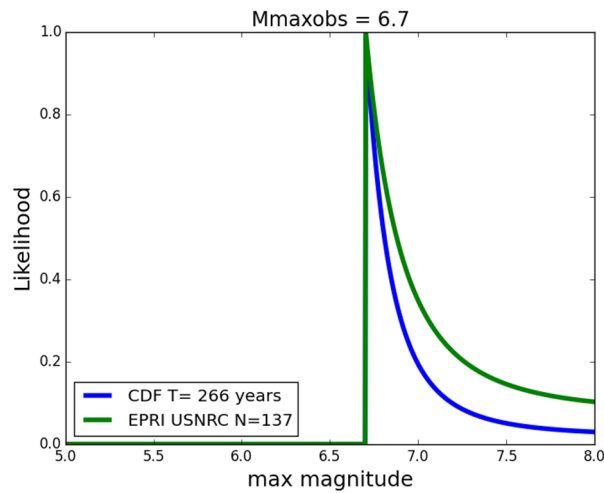
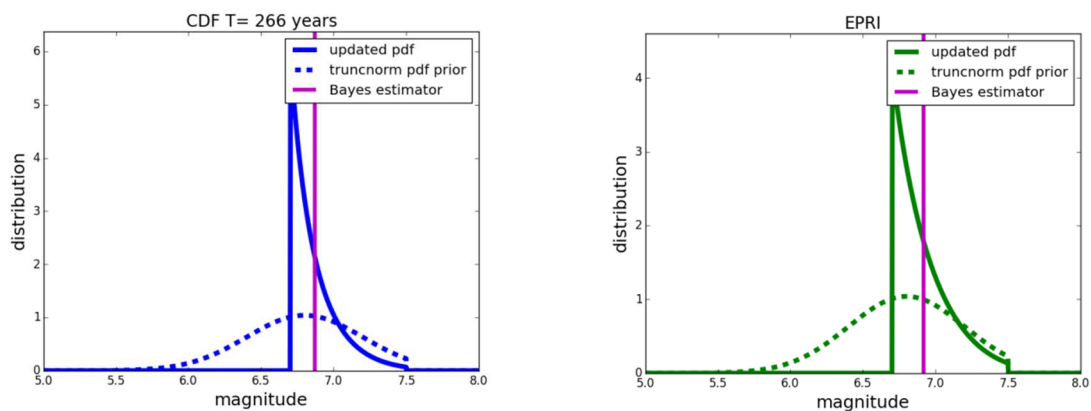


**Figure 25:** Regions for the evaluation of completeness periods, from GEOTER (CEIDRE-TEGG 2017)



**Table 13** Completeness periods determined for mountainous domains (CEIDRE\_TEGG 2017)

LowerMw	UpperMw	YEAR	MIN YEAR	MAX YEAR
1.0	1.5	2014	2013	2015
1.5	2.0	2005	2000	2008
2.0	2.5	1978	1975	1980
2.5	3.0	1965	1960	1975
3.0	3.5	1965	1955	1975
3.5	4.0	1850	1825	1875
4.0	4.5	1800	1750	1850
4.5	5.0	1800	1750	1850
5.0	5.5	1800	1750	1850
5.5	7.5	1800	1750	1850


**Figure 26:** Comparison of likelihood functions from the EPRI method (green,  $N = 137$  events) and the proposed method (blue,  $T = 266$  years).

**Figure 27:** Comparison of the posterior distributions (solid lines) from the EPRI method (right) and the proposed method (left). The prior (dotted lines) is the same in both cases. The Bayes estimator is here the posterior mean.

**Table 14:** Statistics of the posterior distribution of  $m_{max}$  with and without truncation of the Gaussian prior distribution: mean, median and 5%, 95% fractiles

Method	Mean	Median	5% CI	95% CI
<b>T (new approach)</b> no truncation	6,87	6,82	6,71	7,21
	6,88	6,82	6,71	7,24
<b>N (EPRI)</b> no truncation	6,92	6,86	6,71	7,29
	6,93	6,87	6,71	7,35

**Figure 26** compares the likelihood functions corresponding to the EPRI method (green,  $N = 137$  events) and the proposed method (blue,  $T = 266$  years) based on the CDF of extremes. As expected, the latter likelihood function allows for the introduction of a greater amount of information (completeness of  $m_{maxobs}$  instead of the different completeness for the smaller magnitudes) leads to a likelihood more centered around the observed  $m_{max}$ . Obviously, the longer the observation, the more likely it is that  $m_{maxobs}$  is the true  $m_{max}$ : for an infinite duration, the whole population has been observed and  $m_{maxobs}$  equals  $m_{max}$ .

**Figure 27** compares the posterior distributions obtained with the EPRI method (right figure) and the proposed method (left figure). The prior distributions are the same in both cases. The Bayes estimator in the figure is the posterior mean.

The **Table 14** summarizes the results by some statistics of the posterior distribution of  $m_{max}$  with and without truncation of the Gaussian prior distribution. In particular, we compare mean, median and 5%, 95% confidence intervals (CI) of the updated  $m_{max}$  distribution. The updated mean value of the  $m_{max}$  distribution is around  $Mw = 6.9$  for both methods. In agreement with the previous observations regarding the likelihood (**Figure 26**), the proposed approach reduces the 95% confidence interval of the posterior distribution. The truncated prior and the untruncated prior distributions provide very similar results which suggests that the latter can be used.

## Accounting for uncertainty in the data from FCAT17 catalogue

### a) Uncertainty of recurrence parameters and completeness

We consider uncertainty on the recurrence parameters according to the joint distribution given by equations (30) and (31). We furthermore assume a uniform distribution for the duration of completeness  $T$ , with the interval  $\bar{T} \pm 50$  years.

**Figure 28** compares the likelihood functions from the EPRI method ( $N = 137$  events) and the proposed method with and without considering the uncertainties. The likelihood function with uncertainties on GR parameters and completeness shown in the figure is the “marginal” likelihood calculated as:

$$L(obs|m_{max}) = \int L(obs|m_{max}, \beta, \lambda_0, T) f(T) f(\beta, \lambda_0) dT d\beta d\lambda_0 \quad (32)$$

The results show that the uncertainty has no considerable difference in the mean likelihood and thus the resulting posterior distribution.

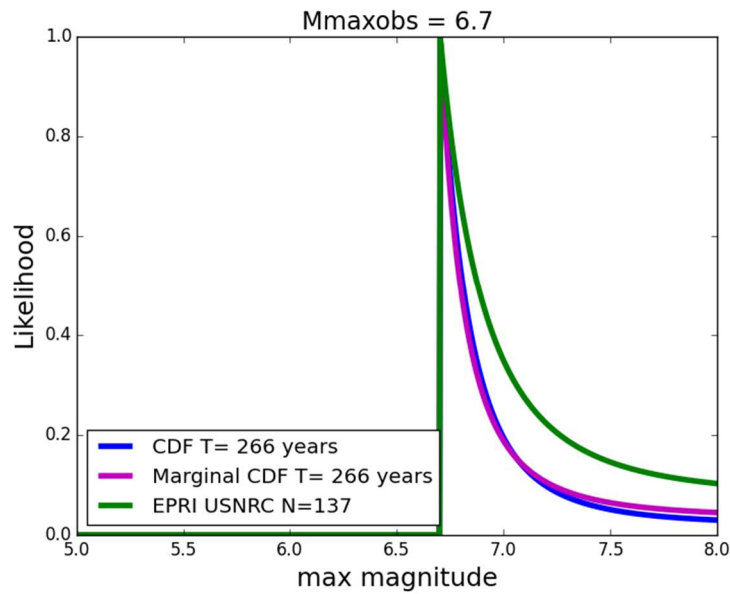


**Figure 28:** Comparison of likelihood functions from the EPRI method (green,  $N = 137$  events) and the proposed method with (marginal distribution, magenta) and without (blue) uncertainties on GR parameters and duration.

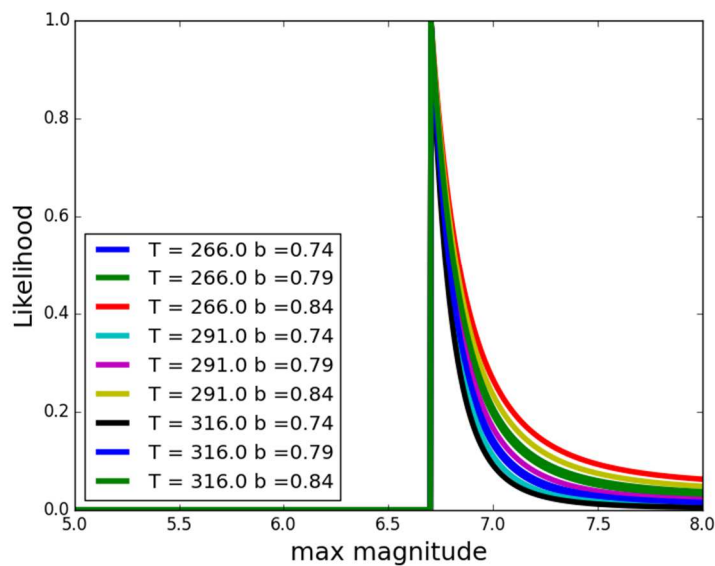


**Figure 29:** Illustration of likelihood functions obtained when accounting for uncertainty in completeness and b-value.

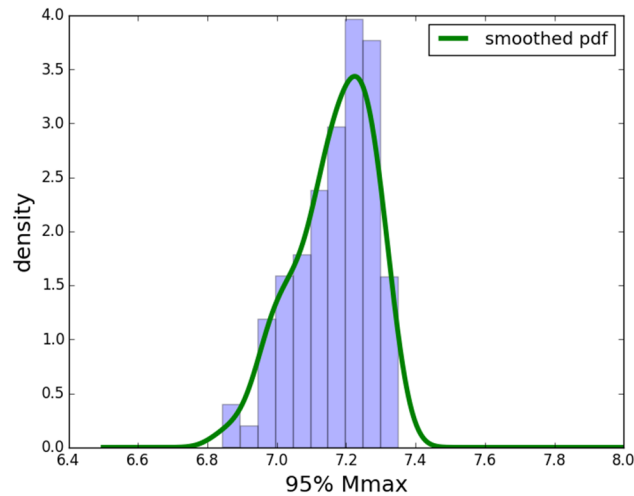


**Figure 30:** Histogram of sample of 95% confidence value of  $m_{\max}$  obtained by sampling the uncertain GR b-parameter and the completeness duration T. This gives a coefficient of variation of  $COV = 1.5\%$  and Mean = 7.17.

Secondly, we propagate uncertainty by Monte Carlo simulation using Latin Hypercube Sampling (LHS) technique. **Figure 29** illustrates the variability of the likelihood functions obtained when considering variations in completeness and b-value. Only part of the whole set of likelihood functions used in the Monte Carlo simulation is shown to keep the figure comprehensive. **Figure 30** shows the histogram of the resulting sample of the 95% confidence value of  $m_{\max}$  obtained by sampling the uncertain parameters. The coefficient of variation, defined as the ratio between the standard deviation and mean, is  $COV = 1.5\%$  for a mean value (of the 95% confidence  $m_{\max}$ ) of  $Mw = 7.17$  and mode (peak of the posterior distribution) of around  $Mw = 7.2$ . We recall here that the 95% value was  $Mw = 7.21$  in the previous analyses without parameter uncertainty, as reported in **Table 11**. The coefficient of variation is very low (1.5%) and indicates that results are robust with respect to uncertainties. However, in the PSHA, the epistemic parameters uncertainty could be considered through the std of the posterior distribution.

#### b) Uncertainty related recurrence parameters and $m_{\max\text{obs}}$

We consider the uncertainties related to the GR parameters as described before and a Gaussian error term for  $m_{\max\text{obs}}$  with a std = 0.2. Possible correlation between the GR parameters and  $m_{\max\text{obs}}$  has been neglected at this stage since no information was available.

**Figure 31** compares the likelihood functions from the EPRI method ( $N = 137$  events) and the proposed method with and without considering the latter uncertainties. The likelihood function with uncertainties on GR parameters and  $m_{\max\text{obs}}$  shown **Figure 30** is the “marginal” likelihood calculated as:

$$L(\text{obs}|m_{\max}) = \int L(\text{obs}|m_{\max}, \beta, \lambda_0) f(\beta, \lambda_0, m_{\max\text{obs}}) d m_{\max\text{obs}} d\beta d\lambda_0 \quad (33)$$

The figure shows that the uncertainty enlarges the peak of the likelihood function and makes it less sharp around  $m_{\max\text{obs}}$ . The uncertainty related to  $m_{\max\text{obs}}$  (the true  $m_{\max\text{obs}}$  could be smaller or larger than the observed  $m_{\max\text{obs}}$ ) also implies that  $m_{\max}$  could also be smaller than the value in the catalogue.

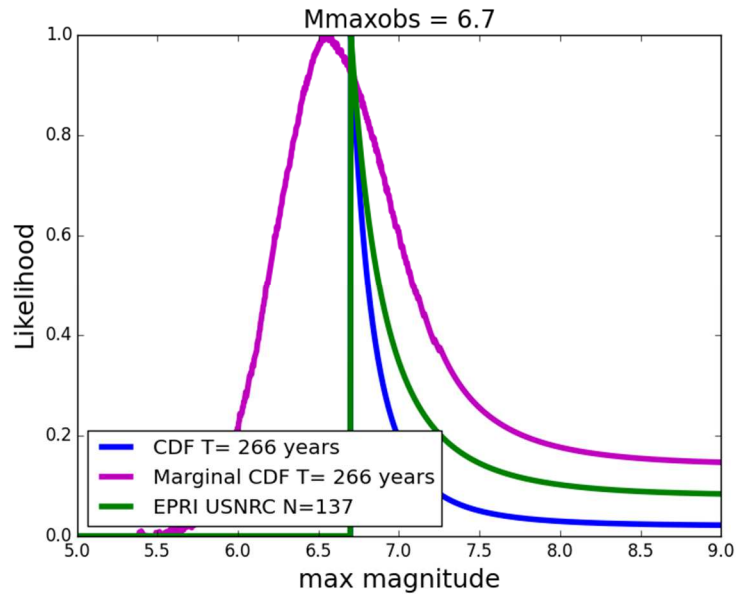


**Figure 31:** Comparison of likelihood functions from the EPRI method (green,  $N = 137$  events) and the proposed method without (blue) and with (marginal distribution, magenta) uncertainties on GR parameters and  $m_{\max\text{obs}}$ .

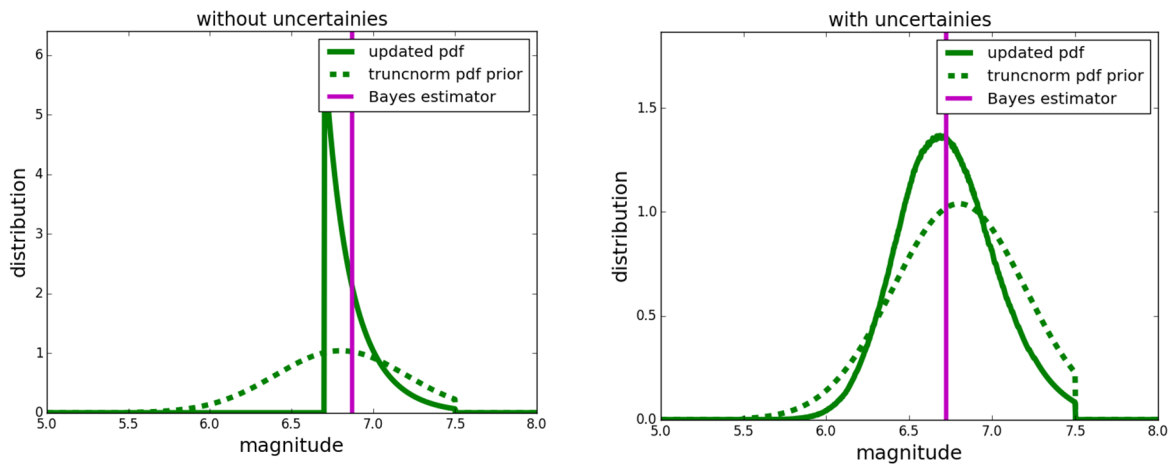


**Figure 32:** Comparison of the posterior distributions (solid lines) with (right) and without (left) considering uncertainty in the likelihood function. The prior (dotted lines) is the same in both cases. The Bayes estimator is here the posterior mean.

**Table 15:** Statistics of the posterior distribution of  $m_{max}$  with and without considering uncertainties on GR parameters and  $m_{maxobs}$  for truncated and not truncated Gaussian prior distribution: mean, median and 5%, 95% fractiles.

Method	Mean	Median	5% CI	95% CI
<b>No uncertainties no truncation</b>	6,87	6,82	6,71	7,21
	6,88	6,82	6,71	7,24
<b>With uncertainties (mean and std) no truncation</b>	6.72	6.71	6.26	7.23
	6.74	6.71	6.26	7.27

The **Table 15** shows the same results as **Table 14** but now the cases where the likelihood function is computed with and without considering uncertainty, and are then compared. The truncated prior and the untruncated prior distributions provide again very similar results. The value  $m_{max}$  has to be known in order to pick the correct mean value in **Figure 22**, but in a realistic case it is not known from the beginning. An iterative procedure is used where the initial value for the mean of the distribution (bias) is chosen according to the results without considering uncertainty. It is then updated to be in agreement with the new estimation of  $m_{max}$ . **Figure 32** compares the posterior distributions obtained with (right figure) and without (left figure) considering uncertainties in the proposed method. The prior distributions are the same in both cases. The Bayes estimator in the figure is the posterior mean. The left curves are the same as the ones shown on the left of **Figure 27**.

The results highlight that the uncertainty on  $m_{maxobs}$  and the GR parameters can be integrated in the updating procedure in a straightforward way. The simulated catalogues allowed for evaluating the bias (mean) and the std of the distribution of the difference between the true and the observed  $m_{maxobs}$ .

For simplicity's sake, we have assumed a Gaussian distribution to represent uncertainty related to  $m_{maxobs}$ . Figure suggests that the distribution is not perfectly symmetric and that another distribution might be more accurate. This topic could not be fully addressed here and will be the object of further improvements of the approach.

## 5. Conclusion and Perspectives

The most commonly used recurrence model is the GR law assuming Poissonian occurrence of earthquakes. In this framework, the maximum magnitude  $m_{max}$  as well as its probability distribution (epistemic uncertainty) can be estimated by Bayesian updating using the analytical expressions of the extreme value distribution. The approach remains applicable when other distributions than the GR law are assumed since the analytical expressions can be derived for any distribution as long as Poisson occurrence is assumed. In the Bayesian approach, the information from similar tectonic zones and expert judgment is introduced by a prior distribution of the maximum magnitude.

We have proposed a new method that combines the distribution of extreme values of the truncated GR law with the Bayesian updating approach. The method constitutes an improvement of former developments by EPRI, see Johnston (1994), and further promoted by USNRC (2012). Indeed, the duration-based formulation of the likelihood proposed here performs slightly better than the EPRI approach because the completeness period of  $m_{maxobs}$  is longer than for  $m_{min}$ . Regarding the time intervals used for the derivation of the extreme value distribution, the analyses showed that the same result is obtained when considering a set of time intervals and their maximum magnitudes or when

considering only one time interval and the associated maximum. As for the EPRI method, the approach also allows addressing the case where  $m_{\max\text{obs}}$  outside its completeness interval. The analyses conducted in this report with simulated catalogues demonstrated the capability of the Bayesian updating approach to correctly estimate  $m_{\max}$ . The proposed method is more rigorous and outperforms the EPRI/USNRC Bayesian updating approach. Only the completeness period of  $m_{\max\text{obs}}$  is required, so that there is no need to determine and use the exact completeness periods for magnitude bins of smaller events and to introduce the associated uncertainties. This makes the approach easy to implement and to apply. Eventually, simulated catalogues demonstrate the possibility to estimate  $m_{\max}$  with the proposed method and for periods of observation available in France.

For the simulated catalogues, magnitude uncertainty has been considered assuming small, moderate and high uncertainty scenarios. The smallest std of 0.1 corresponds to the magnitude uncertainty indicated in the experimental ground motion database RESORCE. The uncertainty related to the more ancient earthquakes is (unavoidably) much higher. According to FCAT17, large uncertainties with standard deviations of up to around 0.5 are present in the historical part of the catalogue. The analyses with the simulated catalogues highlighted and explained the bias in the estimations introduced by the magnitude uncertainty ( $m_{\max}$  is overestimated in the mean). This issue has been addressed by developing a new likelihood function accounting for uncertainty related to the GR parameters as well as the maximum observed magnitude. By this approach, the uncertainty on  $m_{\max\text{obs}}$  and the GR parameters could be integrated in the updating procedure in a straightforward way. The simulated catalogues allowed for evaluating the bias (mean) and the std of the distribution of the difference between the true and the observed  $m_{\max\text{obs}}$ .

In the present work, the catalogues are simulated using the truncated GR law which can be considered as a favorable case. Indeed, the true distribution of magnitudes is not known and might differ from this model. Even if the distribution of magnitudes is well represented by the GR law, it is clear that this is only an approximation of the real law. The robustness of the methodology could be assessed by simulating catalogues with other plausible distributions. This will be addressed in a further work.

The direct estimation of the maximum magnitude by the asymptotic GEV and GPD distributions without hypothesis on the model avoids any further model assumption but comes at the cost of more data to obtain the same precision. Moreover, the resulting estimates might not in agreement with the subsequent engineering analyses if the truncated GR model is used in the PSHA software.

Further developments concern the analyses of alternative magnitude frequency distributions that might be in better agreement with data and/or less sensitive to  $m_{\max}$ . The results were insensitive to the choice of prior distribution, but it is important to pay further attention to the development of the prior and to conduct further sensitivity analyses. It was not possible in the framework of this study to determine the completeness periods of  $m_{\max\text{obs}}$  for all macrozones. This, and the application to other macrozones, will be the object of an update of this report.

## 6. References

Ameri, G. (2014) INTEGRATION OF SIGMA IMPROVEMENT FOR PSHA AND SENSIBILITY STUDIES (INTERMEDIATE RESULTS). Rapport SIGMA-2014-D4-138, Sections 4, 5 & Annexe 4.

Ameri G., Baumont D., Gomes C., Le Dortz, Le Goff, Martin, Secanell (2015). On the choice of maximum earthquake magnitude for seismic hazard assessment in metropolitan France – insight from the Bayesian approach. Colloque AFPS, Paris.

Anderson, J. G., 1979. Estimating the seismicity from geological structure for seismic risk studies, Bull. seism. SOC. Am., 69, 135-158;

I. Zentner - Bayesian estimation of the maximum magnitude  $M_{\max}$  based on the statistics of extremes -  
SIGMA-2-2018-D5-004

Beirlant, J., Goegebeur, Y., Segers, J., and Teugels, J. (2004). *Statistics of Extremes: Theory and Applications*. Probability and Statistics. Wiley.

Burton, Makropoulos (1985). Seismic Risk of Circum-Pacific Earthquakes: II. Extreme Values Using Gumbel's Third Distribution and the Relationship with Strain Energy Release. *Pure and Applied Geophysics* 123(6), Birkhäuser Verlag, Basel, 849-869.

Campbell KW. (1982), Bayesian analysis of extreme earthquake occurrences. Part I. Probabilistic hazard model. *Bulletin of the Seismological Society of America* 72(5):1689-1705.

Campbell KW. (1983) Bayesian analysis of extreme earthquake occurrences. Part II. Application to the San Jacinto fault zone of Southern California. *Bulletin of the Seismological Society of America* 73(4):1099-1115.

CEIDRE-TEGG (2017). Modèle Probabiliste d'aléa sismique pour le territoire Français. Report D309517027095

Coles, Stuart (2001). *An Introduction to Statistical Modeling of Extreme Values*. Springer-Verlag. ISBN 1-85233-459-2.

Cornell, C.A. (1994). Statistical analysis of maximum magnitudes. In: *The Earthquakes of Stable Continental Regions, Vol. 1. Assessment of Large Earthquake Potential*, Electric Power Research Institute, Palo Alto, 5.1–5.27.

Epstein B., Lomnitz C. (1966). A model for the occurrence of large earthquakes, *Nature* 211, 954-956.

Holschneider M., Zöller G., Hainzl S. (2011). Estimation of the Maximum Possible Magnitude in the Framework of a Doubly Truncated Gutenberg–Richter Model. *Bulletin of the Seismological Society of America*, 101 (4) 1649-1659.

Holschneider, M., G. Zöller, R. Clements, and D. Schorlemmer (2014), Can we test for the maximum possible earthquake magnitude? *J. Geophys. Res. Solid Earth*, 119, 2019–2028, doi:[10.1002/2013JB010319](https://doi.org/10.1002/2013JB010319).

Jaynes, E.T. (2007). *Probability Theory: The Logic of Science* (5. print. ed.). Cambridge Univ. Press.. ISBN 978-0-521-59271-0.

Johnston (1994). The stable continental region earthquake database. In: *The Earthquakes of Stable Continental Regions, Vol. 1. Assessment of Large Earthquake Potential*, Electric Power Research Institute, Palo Alto, 3.1–3. 75.

Kagan, Y. Y., and D. D. Jackson (2000). Probabilistic forecasting of earthquakes, *Geophysical Journal International* 143, 438–453.

Kijko A. (2012). On Bayesian procedure for maximum earthquake magnitude estimation. *Research in Geophysics* 2(7).

Kijko, A. & Singh, M. (2011). Statistical tools for maximum possible earthquake magnitude estimation. *Acta Geophys.* 59: 674.

Kijko (2009). On Bayesian procedure for maximum earthquake magnitude estimation. *Research in Geophysics* 2012 volume 2.

Kijko, A. (2004). Estimation of the Maximum Earthquake Magnitude,  $m_{max}$ . *Pure Appl. Geophys* 161(1655), doi:10.1007/s00024-004-2531-4.

Knopoff L., Y. Kagan (1977). *Analysis of the theory of extremes as applied to earthquake problems*, *Journal of Geophysical Research* 82(36).

Koravos G., Main I.G., Tsapanos T.M., Musson R.W. (2003). Maximum earthquake magnitudes in the Aegean area constrained by tectonic moment release. *Geophysical Journal International* 152, 94-112.



Lomnitz-Adler, Lomnitz (1979). A modified form of the Gutenberg-Richter magnitude-frequency relation. *Bulletin of the Seismological Society of America* 96(4).

Main, I.G. & P.W. Burton (1984). Information theory and the earthquake frequency-magnitude distribution, *Bull. Seismol. Soc. Am.* 74, 1409-1426.

Manchuel K., P. Traversa D. Baumont, M. Cara E. Nayman, C. Durouchoux1 (2017). The French seismic CATalogue (FCAT-17). *Bull Earthquake Eng.* DOI 10.1007/s10518-017-0236-1.

Nordquist, J.N. (1945). Theory of largest value applied to earthquake magnitudes. *Trans. Am. Geophys. Union* 26(29), 29-31.

PEGASOS Project (2004). Final Report, Volume 1.

Pisarenko, V.F., Sornette, A., Sornette, D., Rodkin, M.V. (2014). Characterization of the Tail of the Distribution of Earthquake Magnitudes by combining the GEV and GPD descriptions of Extreme Value Theory. *Pure Appl. Geophys.* 171, 1599-1624.

Pisarenko V.F., Sornette, A., Sornette, D., Rodkin, M.V. (2008). New approach to the characterization of  $M_{max}$  and the tail of the distribution of earthquake magnitudes. *Theory. Pure Appl. Geophys.* 165, 847-888.

Pisarenko V.F., Sornette D. (2003). Characterization of Frequency of Extreme Earthquake Events by the Generalized Pareto Distribution. *Pure Appl. Geophys.* 160, 2343-2364.

Pisarenko, V.F., Lyubushin, A.A., Lysenko, V.B., Golubeva T.B. (1996). Statistical estimation of seismic hazard parameters: Maximum possible magnitude and related parameters *Bulletin of the Seismological Society of America* 86(3), 691-700.

Raschke M. (2016). Comment on Pisarenko et al. "Characterization of the Tail of the Distribution of Earthquake Magnitudes by Combining the GEV and GPD Descriptions of Extreme Value Theory". *Pure Appl. Geophys.* 173(2), 701-707.

Raschke M. (2012), Inference for the truncated exponential distribution. *Stochastic Environmental Research and Risk Assessment* 26(1), 127-138.

Rong Y., Bird P., Jackson D.D. (2017). Earthquake potential and magnitude limits in Southern Europe. *Proceedings of WCEE, Santiago, Chile.*

Stevens V. L., J. P. Avouac (2017). Determination of  $M_{max}$  from Background Seismicity and Moment Conservation. *Bulletin of the Seismological Society of America*; 107 (6): 2578-2596.

USNRC (2012). Central and Eastern United States Seismic Source Characterization for Nuclear Facilities. Technical Report. EPRI, Palo Alto, CA, U.S. DOE, and U.S. NRC.

Vanneste K., Vleminckx B., Stein S., Camelbeeck T. (2016). Could  $M_{max}$  Be the Same for All Stable Continental Regions? *Seismological Research Letters* 87(5), 1214-1223.

Wheeler R.L. (2016). Maximum Magnitude ( $M_{max}$ ) in the Central and Eastern United States for the 2014 U.S. Geological Survey Hazard Model. *Bulletin of the Seismological Society of America* 106 (5) 2154-2167; DOI: 10.1785/0120160048.

Wheeler (2009). Methods for  $M_{max}$  estimation East of the Rocky Mountains. USGS report prepared for USNRC.

Zöller G., Hainzl S. (2007). Recurrence Time Distributions of Large Earthquakes in a Stochastic Model for Coupled Fault Systems: The Role of Fault Interaction *Bulletin of the Seismological Society of America*.

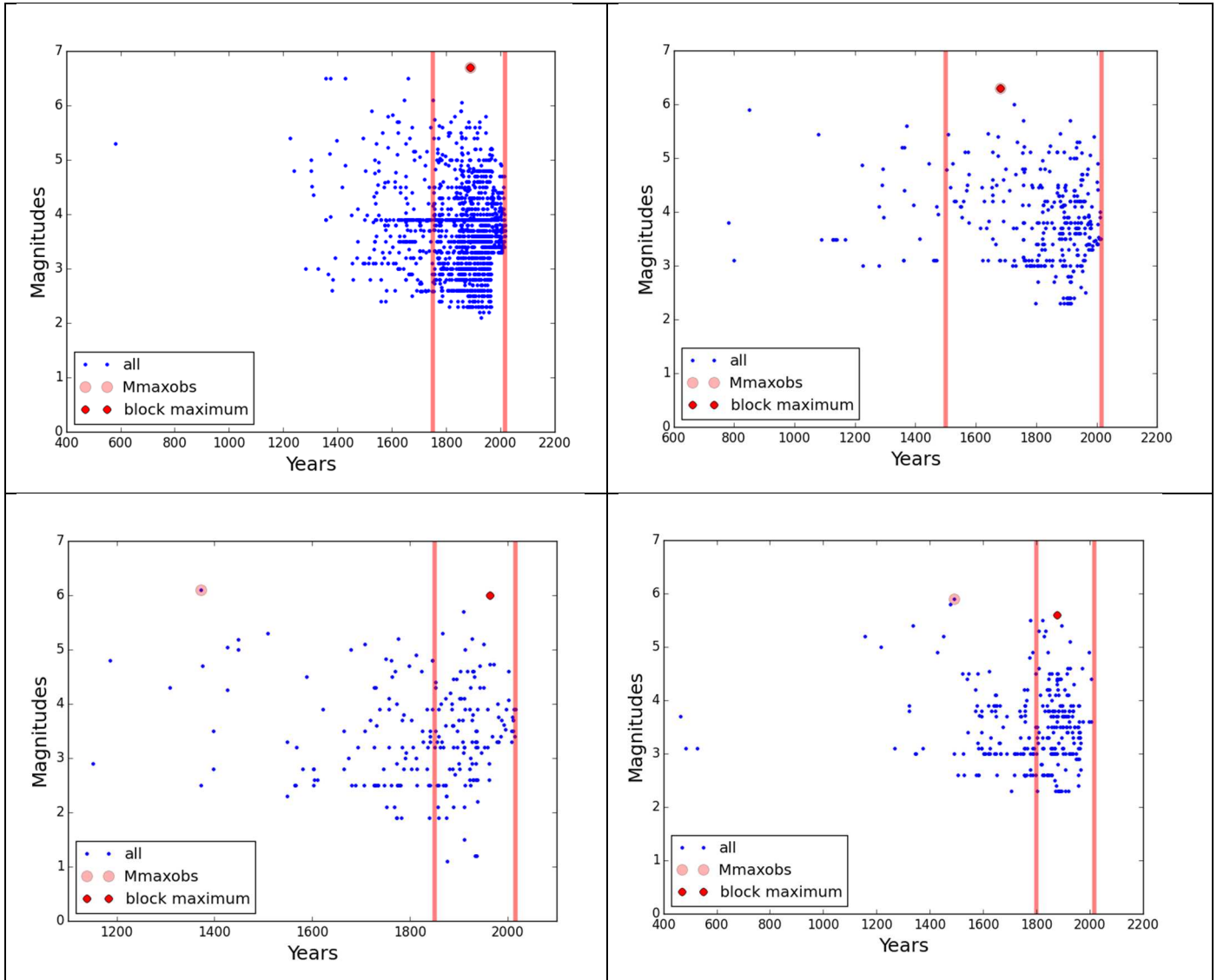
Zöller G., Holschneider M., Hainzl S. (2014). The Largest Expected Earthquake Magnitudes in Japan: The Statistical Perspective. *Bulletin of the Seismological Society of America*, 104(2) 769-779.

Zöller G., Holschneider M., Hainzl S. (2013). The Maximum Earthquake Magnitude in a Time Horizon: Theory and Case Studies. *Bulletin of the Seismological Society of America*, 103(2A) 860-875.

Zöller, Holschneider (2016). The Earthquake History in a Fault Zone Tells Us Almost Nothing about  $m_{max}$ . *SRL* 87(1).

## APPENDIX 1

Visualization of the data from all 6 macrozones.



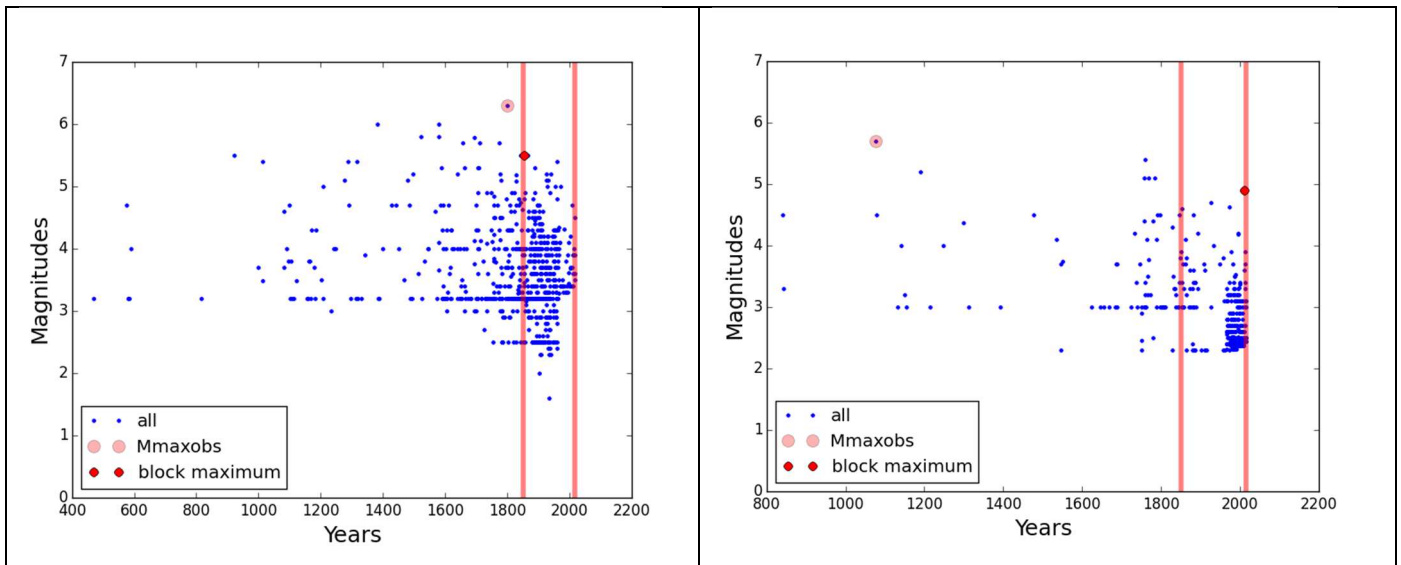


**Figure A1:** From left top to right bottom: data from macrozone D1 to D6, the red vertical lines show the approximate intervals of completeness for  $m_{\text{maxobs}}$  that can be considered for the updating.

## APPENDIX 2

### GR law in log10 base

The Gutenberg-Richter law (1944) represents the annual number of earthquakes larger than a magnitude  $m$ . The relation initially proposed by the authors in base log10 reads:

$$\log_{10} \lambda(M > m) = a - bm$$

With constants  $a$  (global rate of earthquakes in the considered region) and  $b$  (ratio between earthquakes with large and small magnitude, typical values are close to 1). For simplicity's sake, we write  $\lambda_m = \lambda(M > m)$ . This allows for expressing the cumulative distribution function of earthquakes with magnitude larger than  $m_{min}$  as:  $F_M(m) = 1 - 10^{-b(m-m_{min})}$  for  $m > m_{min}$  such that the distribution of magnitudes reads:

$$f_M(m) = b \ln(10) 10^{-b(m-m_{min})} \text{ for } m > m_{min}.$$

Introducing an upper magnitude  $m_{max}$ , we have  $F_m(m) = \frac{\lambda_{m_{min}} - \lambda_m}{\lambda_{m_{min}} - \lambda_{m_{max}}}$  and the distribution of magnitudes reads:

$$f_M(m) = \frac{b \ln(10) 10^{-b(m-m_{min})}}{1 - 10^{-b(m_{max}-m_{min})}} \text{ for } m_{min} < m < m_{max}.$$

With  $a^x = e^{x \ln(a)}$  we can write  $\lambda(M > m) = 10^{a-bm} = e^{(a-bm) \ln(10)}$  such that  $\lambda(M > m) = e^{\alpha - \beta m}$  with  $\beta = b \ln(10)$  and  $\alpha = a \ln(10)$ .